Ground states and dynamics of rotating Bose-Einstein condensates

Weizhu Bao[1]

Department of Mathematics and Center for Computational Science and Engineering, National University of Singapore, Singapore 117543.
bao@cz3.nus.edu.sg

Abstract

In this paper, we review the mathematical and numerical studies of ground states and dynamics in rotating Bose-Einstein condensates (BEC). We start from the three-dimensional (3D) Gross-Pitaevskii equation (GPE) with an angular momentum rotation term, scale it to obtain a four-parameter model, reduce it to a 2D GPE in the limiting regime of strong anisotropic confinement and present its semiclassical scaling and geometrical optics. We discuss existence/nonexistence problem for ground states depending on the angular velocity. We examine the conservation of the angular momentum expectation and the condensate width and analyze the dynamics of a stationary state with a shift in its center. Finally, numerical methods for computing ground state and dynamics of rotating BEC are reviewed and some numerical results are reported.

Key Words: rotating Bose-Einstein condensate, Gross-Pitaevskii equation, ground state, symmetric state, central vortex state, time splitting, angular momentum rotation, continuous normalized gradient flow, energy, chemical potential.

1 Introduction

Since its realization in dilute bosonic atomic gases [7, 23], Bose-Einstein condensation (BEC) of alkali atoms and hydrogen has been produced and studied extensively in the laboratory [1], and has permitted an intriguing glimpse into the macroscopic quantum world. In view of potential applications [38, 63, 64], the study of quantized vortices, which are well-known signatures of superfluidity, is one of the key issues. In fact, bulk superfluids are distinguished from normal fluids by their ability to support dissipationless flow. Such persistent currents are intimately related to the existence of quantized vortices, which are localized phase singularities with integer topological charge [39]. The superfluid vortex is an example of a topological defect that is well known in superconductors [52] and in liquid helium [33]. The occurrence of quantized vortices in superfluids has been the focus of fundamental theoretical and experimental work [33]. Different research groups have obtained quantized vortices in BEC experimentally, e.g. the JILA group [35, 57], the ENS group [56] and the MIT group [1, 32]. Currently, there are at least two typical ways to generate quantized vortices from BEC ground state: (i) impose a laser beam rotating with an angular velocity on the magnetic trap holding the atoms to create a harmonic anisotropic potential [51, 3, 76]; or (ii) add to the stationary magnetic trap a narrow, moving Gaussian potential, representing a far-blue-detuned laser [49, 50, 25, 26, 10, 12]. The recent experimental and theoretical advances in exploration of quantized vortices in BEC have spurred great excitement in the atomic physics community and renewed interest in studying superfluidity.

The properties of a BEC in a rotational frame at temperatures T much smaller than the critical condensation temperature T_c are usually well modeled by a nonlinear Schrödinger equation (NLSE) for the macroscopic wave function known as the Gross-Pitaevskii equation (GPE) [60, 61, 52], which incorporates the trap potential, rotational frame, as well as the interactions among the atoms. The effect of the interactions is described by a mean field which leads to a nonlinear term in the GPE. The cases of repulsive and attractive interactions - which can both be realized in the experiment - correspond to defocusing and focusing nonlinearities in the GPE, respectively.

There has been a series of recent analytical and numerical studies of ground states in rotating BEC. For example, Aftalion and Du [3], Aftalion and Riviere [5] studied numerically and asymptotically ground state, critical angular velocity and energy diagram in the Thomas-Fermi (TF) or semiclassical regime, Aftalion and Danaila [6] and Modugno et al. [59] reported bent vortices, e.g. S-shaped vortex and U-shaped vortex, numerically in cigar-shaped condensation and compared with experimental results [66], Garcia-Ripoll and Perez-Garcia [45, 44, 47], Bao and Zhang [21] studied stability of the central vortex, Tsubota et. al [75] reported vortex lattice formation, Bao et al. [9, 20] presented a continuous normalized gradient flow with backward Euler finite difference discretization to compute ground state, provided asymptotics of the energy and chemical potential of the ground state in the semiclassical regime and showed that the ground state is a global minimizer of the energy functional over the unit sphere and all excited states are saddle points in the linear case. Moreover, Svidzinsky and Fetter [72] have studied dynamics of a vortex line depending on its curvature. For an analysis of the GP-functional in a rotational frame, we refer to [67]. For a numerical and theoretical review of quantized vortices, we refer to [39] and the recent book [61].

In order to study effectively the dynamics of BEC, especially in the strong repulsive interaction regime, an efficient and accurate numerical method is one of the key issues. For non-rotating BEC, many numerical methods were proposed in the literatures. For example, Bao et al. [12, 17, 21] proposed a fourth-order time-splitting sine or Fourier pseudo-spectral (TSSP) method, and Bao and Shen [17] presented a fourth-order time-splitting Laguerre-Hermite (TSLH) pseudo-spectral method for GPE when the external trapping potential is radially or cylindrically symmetric in 2D or 3D. The key ideas for the numerical methods in [12, 11, 21, 17, 14, 15] are based on: (i) a time-splitting technique is applied to decouple the nonlinearity in the GPE [12, 11, 14, 15]; (ii) proper spectral basis functions are chosen for a linear Schrödinger equation with a potential such that the ODE system in phase space is diagonalized and thus can be integrated exactly [12, 17]. These methods are explicit, unconditionally stable, of spectral accuracy in space and fourth-order accuracy in time. Thus they are very efficient and accurate for computing the dynamics of non-rotating BEC in 3D [13] and for multi-component [18], which are the very challenging problems in numerical simulation of BEC. Some other numerical methods for non-rotating BEC include finite difference method [27, 58], particle-inspired scheme [28, 58] and Runge-Kutta pseudo-spectral method [58]. Due to the appearance of the angular momentum rotation term in the GPE, new numerical difficulties must be overcome in designing efficient and accurate numerical methods for rotating BEC. Currently, the numerical methods used in the physics literature for studying dynamics of rotating BEC remain limited [3, 51], and they usually are low-order finite difference methods. Recently, some efficient and accurate numerical methods were designed for computing dynamics of rotating BEC. For example, Bao, Du and Zhang [10] proposed a numerical method for computing dynamics of rotating BEC by applying a time-splitting technique for decoupling the nonlinearity in the GPE and adopting the polar coordinates or cylindrical coordinates so as to make the coefficient of the angular momentum rotation term constant. The method is time reversible, time transverse invariant, unconditionally stable, implicit in 1D but can be solved very efficiently, and conserves the total density. It is of spectral accuracy in transverse direction, but usually of second or fourth-order accuracy in radial direction. Zhang and Bao [77] used the leap-frog spectral method for studying vortex lattice dynamics in rotating BEC in which the Cartesian coordinate is adopted. This method is explicit, time reversible, of spectral accuracy in space and second order accuracy in time. It is stable under a stability constraint for time step [77]. Bao and Wang [19] presented a time-splitting spectral (TSSP) method by applying a time-splitting technique for decoupling the nonlinearity and properly using the alternating direction implicit (ADI) technique for the coupling in the angular momentum rotation term in the GPE. Thus at every time step, the GPE in rotational frame is decoupled into a nonlinear ordinary differential equation (ODE) and two partial differential equations with constant coefficients. This allows them to develop new TSSP methods for computing the dynamics of BEC in a rotational frame. The new numerical method is explicit, unconditionally stable, and of spectral accuracy in space and second order accuracy in time. Moreover, it is time reversible and time transverse invariant, and conserves the position density in the discretized level.

The main aim of this paper is to review the above results and methods for rotating BEC. The paper is organized as follows. In section 2, we take the 3D GPE with an angular momentum term, scale it to get a four parameter model, reduce it to a 2D problem in a limiting regime, present its semiclassical scaling and geometrical optics. In section 3, we discuss existence/nonexistence of the ground state in rotating BEC, provide approximate ground state in limiting parameter regimes. In section 4, we review the continuous normalized gradient flow and its backward Euler finite difference discretization for computing ground and vortex states of rotating BEC and report some numerical results. Some analytical results for dynamics of rotating BEC are reviewed in section 5, and several efficient and accurate numerical methods for computing dynamics of rotating BEC are discussed in section 6. Finally, in section 7, some conclusions are drawn.

2 GPE in a rotational frame

At temperatures T much smaller than the critical temperature T_c [52], a BEC in a rotational frame is well described by the macroscopic wave function $\psi(\mathbf{x},t)$, whose evolution is governed by a self-consistent, mean field nonlinear Schrödinger equation known as the Gross-Pitaevskii equation (GPE) with an angular momentum rotational term [24, 36, 45], (w.l.o.g.) assuming the rotation being around the z-axis:

$$\begin{aligned} i\hbar\frac{\partial\psi(\mathbf{x},t)}{\partial t} &= \frac{\delta E(\psi)}{\delta\psi^*} := H\ \psi \\ &= \left(-\frac{\hbar^2}{2m}\nabla^2 + V(\mathbf{x}) + NU_0|\psi(\mathbf{x},t)|^2 - \Omega L_z\right)\psi(\mathbf{x},t), \end{aligned} \tag{1}$$

where $\mathbf{x}=(x,y,z)^T\in\mathbb{R}^3$ is the spatial coordinate vector, m is the atomic mass, $\hbar$ is the Planck constant, N is the number of atoms in the condensate, Ω is an angular velocity, $V(\mathbf{x})$ is an external trapping potential. When a harmonic trap potential is considered, $V(\mathbf{x})=\frac{m}{2}\left(\omega_x^2x^2+\omega_y^2y^2+\omega_z^2z^2\right)$ with ω_x, ω_y and ω_z being the trap frequencies in x-, y- and z-direction respectively. $U_0=\frac{4\pi\hbar^2a_s}{m}$ describes the interaction between atoms in the condensate with the s-wave scattering length a_s (positive for repulsive interaction and negative for attractive interaction) and

$$L_z = xp_y - yp_x = -i\hbar\left(x\partial_y - y\partial_x\right) \tag{2}$$

is the z-component of the angular momentum $\mathbf{L}=\mathbf{x}\times\mathbf{P}$ with the momentum operator $\mathbf{P}=-i\hbar\nabla=(p_x,p_y,p_z)^T$. The energy functional per particle $E(\psi)$ is defined as

$$E(\psi) = \int_{\mathbb{R}^3} \left[\frac{\hbar^2}{2m} |\nabla \psi|^2 + V(\mathbf{x})|\psi|^2 + \frac{NU_0}{2}|\psi|^4 - \Omega \psi^* L_z \psi \right] d\mathbf{x}. \qquad (3)$$

Here we use f^* denotes the conjugate of a function f. It is convenient to normalize the wave function by requiring

$$\int_{\mathbb{R}^3} |\psi(\mathbf{x},t)|^2 \; d\mathbf{x} = 1. \qquad (4)$$

2.1 Dimensionless GPE in a rotational frame

Under the normalization condition (4), by introducing the dimensionless variables: $t \to t/\omega_m$ with $\omega_m = \min\{\omega_x, \omega_y, \omega_z\}$, $\mathbf{x} \to \mathbf{x} a_0$ with $a_0 = \sqrt{\hbar / m\omega_m}$, $\psi \to \psi / a_0^{3/2}$, $\Omega \to \Omega \omega_m$ and $E(\cdot) \to \hbar \omega_m E_{\beta,\Omega}(\cdot)$, we get the dimensionless GPE

$$\begin{aligned} i\,\frac{\partial \psi(\mathbf{x},t)}{\partial t} &= \frac{\delta E_{\beta,\Omega}(\psi)}{\delta \psi^*} := H\;\psi \\ &= \left(-\frac{1}{2}\nabla^2 + V(\mathbf{x}) + \beta\,|\psi(\mathbf{x},t)|^2 - \Omega L_z \right) \psi(\mathbf{x},t), \end{aligned} \qquad (5)$$

where $\beta = \frac{U_0 N}{a_0^3 \hbar \omega_m} = \frac{4\pi a_s N}{a_0}$, $L_z = -i(x\partial_y - y\partial_x)$, $V(\mathbf{x}) = \frac{1}{2}\left(\gamma_x^2 x^2 + \gamma_y^2 y^2 + \gamma_z^2 z^2\right)$ with $\gamma_x = \frac{\omega_x}{\omega_m}$, $\gamma_y = \frac{\omega_y}{\omega_m}$ and $\gamma_z = \frac{\omega_z}{\omega_m}$, and the dimensionless energy functional per particle $E_{\beta,\Omega}(\psi)$ is defined as

$$E_{\beta,\Omega}(\psi) = \int_{\mathbb{R}^3} \left[\frac{1}{2} |\nabla \psi(\mathbf{x},t)|^2 + V(\mathbf{x})|\psi|^2 + \frac{\beta}{2}\,|\psi|^4 - \Omega \psi^*\, L_z \psi \right] d\mathbf{x}. \qquad (6)$$

In a disk-shaped condensation with parameters $\omega_x \approx \omega_y$ and $\omega_z \gg \omega_x$ ($\Longleftrightarrow$ $\gamma_x = 1$, $\gamma_y \approx 1$ and $\gamma_z \gg 1$ with choosing $\omega_m = \omega_x$), the 3D GPE (5) can be reduced to a 2D GPE with $\mathbf{x} = (x,y)^T$ [12, 8, 18]:

$$i\,\frac{\partial \psi(\mathbf{x},t)}{\partial t} = -\frac{1}{2}\nabla^2 \psi + V_2(x,y)\psi + \beta_2 |\psi|^2 \psi - \Omega L_z \psi, \qquad (7)$$

where $\beta_2 \approx \beta_2^a = \beta\sqrt{\gamma_z / 2\pi}$ and $V_2(x,y) = \frac{1}{2}\left(\gamma_x^2 x^2 + \gamma_y^2 y^2\right)$ [12, 18, 3]. Thus here we consider the dimensionless GPE in a rotational frame in d-dimensions ($d = 2, 3$):

$$i\,\frac{\partial \psi(\mathbf{x},t)}{\partial t} = -\frac{1}{2}\nabla^2 \psi + V_d(\mathbf{x})\psi + \beta_d |\psi|^2 \psi - \Omega L_z \psi, \;\; \mathbf{x} \in \mathbb{R}^d, \;\; t \geq 0, \quad (8)$$

$$\psi(\mathbf{x},0) = \psi_0(\mathbf{x}), \qquad \mathbf{x} \in \mathbb{R}^d; \qquad (9)$$

where $\beta_3 = \beta$ and $V_3(x,y,z) = V(x,y,z)$.

Two important invariants of (8) are the *normalization of the wave function*

$$N(\psi) = \int_{\mathbb{R}^d} |\psi(\mathbf{x},t)|^2 \; d\mathbf{x} \equiv \int_{\mathbb{R}^d} |\psi(\mathbf{x},0)|^2 \; d\mathbf{x} = 1, \qquad t \geq 0 \qquad (10)$$

and the *energy*

$$E_{\beta,\Omega}(\psi) = \int_{\mathbb{R}^d} \left[\frac{1}{2}\left|\nabla\psi(\mathbf{x},t)\right|^2 + V_d(\mathbf{x})|\psi|^2 + \frac{\beta_d}{2}\,|\psi|^4 - \Omega\psi^*\,L_z\psi\right] d\mathbf{x}. \quad (11)$$

2.2 Stationary states

To find a stationary solution of (8), we write

$$\psi(\mathbf{x},t) = e^{-i\mu t}\phi(\mathbf{x}), \quad (12)$$

where μ is the chemical potential of the condensate and ϕ is independent of time. Inserting (12) into (8) gives the following equation for $\phi(\mathbf{x})$

$$\mu\,\phi(\mathbf{x}) = -\frac{1}{2}\Delta\phi(\mathbf{x}) + V_d(\mathbf{x})\,\phi(\mathbf{x}) + \beta_d|\phi(\mathbf{x})|^2\phi(\mathbf{x}) - \Omega L_z\phi(\mathbf{x}),\ \ \mathbf{x}\in\mathbb{R}^d, \quad (13)$$

under the normalization condition

$$\|\phi\|^2 = \int_{\mathbb{R}^d} |\phi(\mathbf{x})|^2\, d\mathbf{x} = 1. \quad (14)$$

This is a nonlinear eigenvalue problem with a constraint and any eigenvalue μ can be computed from its corresponding eigenfunction ϕ by

$$\begin{aligned}\mu &= \mu_{\beta,\Omega}(\phi)\\ &= \int_{\mathbb{R}^d}\left[\frac{1}{2}\left|\nabla\phi(\mathbf{x})\right|^2 + V_d(\mathbf{x})\left|\phi(\mathbf{x})\right|^2 + \beta_d\left|\phi(\mathbf{x})\right|^4 - \Omega\phi^*(\mathbf{x})L_z\phi(\mathbf{x})\right] d\mathbf{x}\\ &= E_{\beta,\Omega}(\phi) + \int_{\mathbb{R}^d}\frac{\beta_d}{2}\left|\phi(\mathbf{x})\right|^4\, d\mathbf{x}. \end{aligned}\quad (15)$$

In fact, the eigenfunctions of (13) under the constraint (14) are the critical points of the energy functional $E_{\beta,\Omega}(\phi)$ over the unit sphere $S = \{\phi\in\mathbb{C}\mid \|\phi\|=1, E_{\beta,\Omega}(\phi)<\infty\}$. Furthermore (13) is the Euler-Lagrange equation of the energy functional (11) with $\psi=\phi$ under the constraint (14).

2.3 Semiclassical scaling and geometrical optics

When $\beta_d \gg 1$, i.e. in a strongly repulsive interacting condensation or in semiclassical regime, another scaling (under the normalization (10) with $\psi=\psi^\varepsilon$) for the GPE (8) is also very useful in practice by choosing $\mathbf{x}\to\varepsilon^{-1/2}\mathbf{x}$ and $\psi=\psi^\varepsilon\,\varepsilon^{d/4}$ with $\varepsilon=\beta_d^{-2/(d+2)}$:

$$\begin{aligned} i\varepsilon\,\frac{\partial\psi^\varepsilon(\mathbf{x},t)}{\partial t} &= \frac{\delta E_{\varepsilon,\Omega}(\psi^\varepsilon)}{\delta(\psi^\varepsilon)^*} := H^\varepsilon\,\psi^\varepsilon\\ &= -\frac{\varepsilon^2}{2}\nabla^2\psi^\varepsilon + V_d(\mathbf{x})\psi^\varepsilon + |\psi^\varepsilon|^2\psi^\varepsilon - \varepsilon\Omega L_z\psi^\varepsilon, \quad \mathbf{x}\in\mathbb{R}^d, \end{aligned}\quad (16)$$

where the energy functional $E_{\varepsilon,\Omega}(\psi^\varepsilon)$ is defined as

$$E_{\varepsilon,\Omega}(\psi^\varepsilon) = \int_{\mathbb{R}^3} \left[\frac{\varepsilon^2}{2}|\nabla\psi^\varepsilon|^2 + V_d(\mathbf{x})|\psi^\varepsilon|^2 + \frac{1}{2}|\psi^\varepsilon|^4 - \varepsilon\Omega(\psi^\varepsilon)^* L_z\psi^\varepsilon\right] d\mathbf{x} \\ = O(1),$$

assuming that ψ^ε is ε-oscillatory and 'sufficiently' integrable such that all terms have $O(1)$-integral. Similarly, the nonlinear eigenvalue problem (13) (under the normalization (14) with $\phi = \phi^\varepsilon$) reads

$$\mu^\varepsilon\phi^\varepsilon(\mathbf{x}) = -\frac{\varepsilon^2}{2}\Delta\phi^\varepsilon + V_d(\mathbf{x})\phi^\varepsilon + |\phi^\varepsilon|^2\phi^\varepsilon - \varepsilon\Omega L_z\phi^\varepsilon, \quad \mathbf{x}\in\mathbb{R}^d, \tag{17}$$

where any eigenvalue μ^ε can be computed from its corresponding eigenfunction ϕ^ε by

$$\mu^\varepsilon = \mu_{\varepsilon,\Omega}(\phi^\varepsilon) = \int_{\mathbb{R}^d} \left[\frac{\varepsilon^2}{2}|\nabla\phi^\varepsilon|^2 + V_0(\mathbf{x})|\phi^\varepsilon|^2 + |\phi^\varepsilon|^4 - \varepsilon\Omega(\psi^\varepsilon)^* L_z\psi^\varepsilon\right] d\mathbf{x} \\ = O(1).$$

Furthermore it is easy to get the leading asymptotics of the energy functional $E_{\beta,\Omega}(\psi)$ in (11) and the chemical potential $\mu_{\beta,\Omega}(\phi)$ in (15) when $\beta_d \gg 1$ from this scaling:

$$E_{\beta,\Omega}(\psi) = \varepsilon^{-1}E_{\varepsilon,\Omega}(\psi^\varepsilon) = O\left(\varepsilon^{-1}\right) = O\left(\beta_d^{2/(d+2)}\right), \tag{18}$$

$$\mu_{\beta,\Omega}(\phi) = \varepsilon^{-1}\mu_{\varepsilon,\Omega}(\phi^\varepsilon) = O\left(\varepsilon^{-1}\right) = O\left(\beta_d^{2/(d+2)}\right), \qquad \beta_d \gg 1. \tag{19}$$

These asymptotic results were confirmed by the numerical results in [16, 20].

When $0 < \varepsilon \ll 1$, i.e. $\beta_d \gg 1$, we set

$$\psi^\varepsilon(\mathbf{x},t) = \sqrt{\rho^\varepsilon(\mathbf{x},t)}\exp\left(\frac{i}{\varepsilon}S^\varepsilon(\mathbf{x},t)\right), \tag{20}$$

where $\rho^\varepsilon = |\psi^\varepsilon|^2$ and S^ε is the phase of the wave-function. Inserting (20) into (16) and collecting real and imaginary parts, we get the transport equation for ρ^ε and the Hamilton-Jacobi equation for the phase S^ε:

$$\partial_t\rho^\varepsilon + \mathrm{div}\,(\rho^\varepsilon\nabla S^\varepsilon) + \Omega\widehat{L}_z\rho^\varepsilon = 0, \tag{21}$$

$$\partial_t S^\varepsilon + \frac{1}{2}|\nabla S^\varepsilon|^2 + V_d(\mathbf{x}) + \rho^\varepsilon + \Omega\widehat{L}_z S^\varepsilon = \frac{\varepsilon^2}{2}\frac{1}{\sqrt{\rho^\varepsilon}}\nabla^2\sqrt{\rho^\varepsilon}, \tag{22}$$

where the operator $\widehat{L}_z = (x\partial_y - y\partial_x)$. Eq. (21) is the transport equation for the atom density and (22) the Hamilton-Jacobi equation for the phase. Furthermore, by defining the current density [20, 15]

$$\mathbf{J}^\varepsilon = \rho^\varepsilon\nabla S^\varepsilon = \varepsilon\,\mathrm{Im}\left((\psi^\varepsilon(\mathbf{x},t))^*\,\nabla\psi^\varepsilon(\mathbf{x},t)\right), \tag{23}$$

we can get the quantum-hydrodynamic Euler system with a third-order dispersion term:

$$\partial_t \rho^\varepsilon + \mathrm{div}\mathbf{J}^\varepsilon + \Omega \widehat{L}_z \rho^\varepsilon = 0, \tag{24}$$

$$\begin{aligned}\partial_t \mathbf{J}^\varepsilon + \mathrm{div}\left(\frac{\mathbf{J}^\varepsilon \otimes \mathbf{J}^\varepsilon}{\rho^\varepsilon}\right) + \nabla P(\rho^\varepsilon) + \rho^\varepsilon \nabla V_d(\mathbf{x}) \\ + \Omega\left(\widehat{L}_z + \mathbf{G}\right)\mathbf{J}^\varepsilon = \frac{\varepsilon^2}{4}\nabla\left(\rho^\varepsilon \nabla^2 \ln \rho^\varepsilon\right),\end{aligned} \tag{25}$$

where $P(\rho) = \frac{\rho^2}{2}$ is the hydrodynamic pressure and the symplectic matrix $\mathbf{G}$ is defined as

$$\mathbf{G} = \begin{pmatrix} 0 & 1 \\ -1 & 0 \end{pmatrix}, \quad \text{for} \quad d = 2, \qquad \mathbf{G} = \begin{pmatrix} 0 & 1 & 0 \\ -1 & 0 & 0 \\ 0 & 0 & 0 \end{pmatrix}, \quad \text{for} \quad d = 3. \tag{26}$$

By formally passing to the limit $\varepsilon \to 0+$ in (21)-(22), we obtain the system

$$\partial_t \rho^0 + \mathrm{div}\left(\rho^0 \nabla S^0\right) + \Omega \widehat{L}_z \rho^0 = 0, \tag{27}$$

$$\partial_t S^0 + \frac{1}{2}\left|\nabla S^0\right|^2 + V_d(\mathbf{x}) + \rho^0 + \Omega \widehat{L}_z S^0 = 0. \tag{28}$$

Similarly, letting $\varepsilon \to 0^+$ in (24)$-$(25), we can formally obtain the following Euler system:

$$\partial_t \rho^0 + \mathrm{div}\mathbf{J}^0 + \Omega \widehat{L}_z \rho^0 = 0, \tag{29}$$

$$\partial_t \mathbf{J}^0 + \mathrm{div}\left(\frac{\mathbf{J}^0 \otimes \mathbf{J}^0}{\rho^0}\right) + \nabla P(\rho^0) + \rho^0 \nabla V_d(\mathbf{x}) + \Omega\left(\widehat{L}_z + \mathbf{G}\right)\mathbf{J}^0 = 0, \tag{30}$$

which is the isotropic Euler system (velocity given by $v^0 = \nabla s^0$) with quadratic pressure-density constitutive relation in the rotational frame. The formal asymptotics is supposed to hold up to caustic onset time!

3 Ground state

The ground state wave function $\phi^g(\mathbf{x}) := \phi^g_{\beta,\Omega}(\mathbf{x})$ of a rotating BEC is found by minimizing the energy functional $E_{\beta,\Omega}(\phi)$ over the unit sphere S:

(I) Find $(\mu^g_{\beta,\Omega}, \phi^g_{\beta,\Omega} \in S)$ such that

$$E^g := E^g_{\beta,\Omega} = E_{\beta,\Omega}(\phi^g_{\beta,\Omega}) = \min_{\phi \in S} E_{\beta,\Omega}(\phi), \quad \mu^g := \mu^g_{\beta,\Omega} = \mu_{\beta,\Omega}(\phi^g_{\beta,\Omega}). \tag{31}$$

Any eigenfunction $\phi(\mathbf{x})$ of (13) under the constraint (14) whose energy $E_{\beta,\Omega}(\phi) > E_{\beta,\Omega}(\phi^g_{\beta,\Omega})$ is usually called as an excited state in the physical literature [61].

Existence/nonexistence results of ground state, depending on the magnitude $|\Omega|$ of the angular velocity relative to the trapping frequencies are known and can be found [67].

3.1 Existence of the ground state when $|\Omega| < \gamma_{xy} := \min\{\gamma_x, \gamma_y\}$

To study the existence of the ground state in rotating BEC, we first present some properties of the energy functional [20]

Lemma 1. *i) In 2D, we have*

$$\begin{aligned} &E_{\beta,-\Omega}(\phi(x,-y)) = E_{\beta,\Omega}(\phi(x,y)), \\ &E_{\beta,-\Omega}(\phi(-x,y)) = E_{\beta,\Omega}(\phi(x,y)), \qquad \phi \in S. \end{aligned} \tag{32}$$

ii) In 3D, we have

$$\begin{aligned} &E_{\beta,-\Omega}(\phi(x,-y,z)) = E_{\beta,\Omega}(\phi(x,y,z)), \\ &E_{\beta,-\Omega}(\phi(-x,y,z)) = E_{\beta,\Omega}(\phi(x,y,z)), \qquad \phi \in S. \end{aligned} \tag{33}$$

iii) In 2D and 3D, we have

$$\begin{aligned} &\int_{\mathbb{R}^d} \left[\frac{1-|\Omega|}{2}\,|\nabla\phi(\mathbf{x})|^2 + \left(V_d(\mathbf{x}) - \frac{|\Omega|}{2}(x^2+y^2)\right)|\phi|^2 + \frac{\beta_d}{2}\,|\phi|^4\right] d\mathbf{x} \le E_{\beta,\Omega}(\phi) \\ &\le \int_{\mathbb{R}^d} \left[\frac{1+|\Omega|}{2}\,|\nabla\phi(\mathbf{x})|^2 + \left(V_d(\mathbf{x}) + \frac{|\Omega|}{2}(x^2+y^2)\right)|\phi|^2 + \frac{\beta_d}{2}\,|\phi|^4\right] d\mathbf{x}. \end{aligned} \tag{34}$$

From this lemma, since $\gamma_y \ge \gamma_x = \gamma_{xy}$ and $\gamma_z > 0$, when $\beta_d \ge 0$ and $|\Omega| < \gamma_{xy}$, we know that the energy functional $E_{\beta,\Omega}(\phi)$ is positive, coercive and weakly lower semicontinuous on S. Thus the existence of a minimum follows from the standard theory [73] and we have

Theorem 1. *i) In 2D, if $\phi_{\beta,\Omega}(x,y) \in S$ is a ground state of the energy functional $E_{\beta,\Omega}(\phi)$, then $\phi_{\beta,\Omega}(x,-y) \in S$ and $\phi_{\beta,\Omega}(-x,y) \in S$ are ground states of the energy functional $E_{\beta,-\Omega}(\phi)$. Furthermore*

$$E^g_{\beta,\Omega} = E^g_{\beta,-\Omega}, \qquad \mu^g_{\beta,\Omega} = \mu^g_{\beta,-\Omega}. \tag{35}$$

ii) In 3D, if $\phi_{\beta,\Omega}(x,y,z) \in S$ is a ground state of the energy functional $E_{\beta,\Omega}(\phi)$, then $\phi_{\beta,\Omega}(x,-y,z) \in S$ and $\phi_{\beta,\Omega}(-x,y,z) \in S$ are ground states of the energy functional $E_{\beta,-\Omega}(\phi)$, and (35) is also valid.

iii). When $\beta_d \ge 0$ and $|\Omega| < \gamma_{xy}$, there exists a minimizer for the minimization problem (31), i.e. there exist ground state.

For understanding the uniqueness question, note that $E_{\beta,\Omega}(\alpha\phi^g_{\beta,\Omega}) = E_{\beta,\Omega}(\phi^g_{\beta,\Omega})$ for all $\alpha \in \mathbb{C}$ with $|\alpha| = 1$. Thus an additional constraint has to be introduced to show uniqueness. For non-rotating BEC, i.e. $\Omega = 0$, the unique positive minimizer is usually taken as the ground state. In fact, the ground state is unique up to a constant α with $|\alpha| = 1$, i.e. density of the ground state is unique, when $\Omega = 0$. For rotating BEC under $|\Omega| < \gamma_{xy}$, several numerical methods were proposed in the literature [3, 20] for computing a minimizer of the minimization problem (31). From the numerical results [3, 20], the density of the ground state may no longer unique when $|\Omega| > \Omega^c$ with Ω^c a critical angular rotation speed.

3.2 Nonexistence of ground states when $|\Omega| > \gamma^{xy} := \max\{\gamma_x, \gamma_y\}$

Denote $\gamma_r := \gamma^{xy}$ and notice $\frac{1}{2}(\gamma_x^2 x^2 + \gamma_y^2 y^2) \le \frac{1}{2}\gamma_r^2 r^2$ with $r = \sqrt{x^2+y^2}$, we have

$$E_{\beta,\Omega}(\phi) \le \frac{1}{2}\int_0^{2\pi}\int_0^\infty \Big[|\partial_r\phi|^2 + \frac{1}{r^2}|\partial_\theta\phi|^2 + \gamma_r^2 r^2|\phi|^2 + \beta_2|\phi|^4 + 2i\Omega\phi^*\partial_\theta\phi\Big] r\, drd\theta, \quad d=2, \tag{36}$$

$$E_{\beta,\Omega}(\phi) \le \frac{1}{2}\int_{-\infty}^\infty\int_0^{2\pi}\int_0^\infty \Bigg[|\partial_r\phi|^2 + \frac{1}{r^2}|\partial_\theta\phi|^2 + |\partial_z\phi|^2 + (\gamma_r^2 r^2 + \gamma_z^2 z^2)|\phi|^2 + \beta_2|\phi|^4 + 2i\Omega\phi^*\partial_\theta\phi\Bigg] r\, drd\theta dz, \qquad d=3, \tag{37}$$

where (r,θ) and (r,θ,z) are polar (in 2D), and resp., cylindrical coordinates (in 3D). In 2D, let

$$\phi_m(\mathbf{x}) = \phi_m(r,\theta) = \phi_m(r)\, e^{im\theta}, \quad \text{with } \phi_m(r) = \frac{\gamma_r^{(|m|+1)/2}}{\sqrt{\pi|m|!}} r^{|m|} e^{-\frac{\gamma_r r^2}{2}}, \tag{38}$$

where m is an integer. In fact, $\phi_m(\mathbf{x})$ is the central vortex state with winding number m of the GPE (8) with $d=2$, $\beta_d = 0$ and $\Omega = 0$. It is very easy to check that ϕ_m satisfies

$$\|\phi_m\| = 2\pi\int_0^\infty |\phi_m(r)|^2\, r\, dr = 1, \qquad m \in \mathbb{Z}, \tag{39}$$

$$\frac{1}{2}\left[-\frac{1}{r}\frac{d}{dr}\left(r\frac{d}{dr}\right) + r^2 + \frac{m^2}{r^2}\right]\phi_m(r) = (|m|+1)\gamma_r\phi_m(r), \ 0<r<\infty. \tag{40}$$

Thus $\phi_m \in S$ and we compute

$$\begin{aligned} E_{\beta,\Omega}(\phi_m(\mathbf{x})) &\le (|m|+1)\gamma_r - \Omega m + \beta_2\pi\int_0^\infty |\phi_m(r)|^4 r\, dr \\ &= (|m|+1)\gamma_r - \Omega m + \frac{\beta_2\gamma_r(2|m|)!}{4\pi(2^{|m|}(|m|!))^2}. \end{aligned} \tag{41}$$

Thus when $|\Omega| > \gamma_r$, we have

$$\begin{aligned} \inf_{\phi\in S} E_{\beta,\Omega}(\phi) &\le \begin{cases} \lim_{m\to\infty} E_{\beta,\Omega}(\phi_m) & \Omega > 0, \\ \lim_{m\to\infty} E_{\beta,\Omega}(\phi_{-m}) & \Omega < 0 \end{cases} \\ &= \lim_{m\to\infty}(\gamma_r - |\Omega|)|m| + \gamma_r + \frac{\beta_2\gamma_r(2|m|)!}{4\pi(2^{|m|}(|m|!))^2} = -\infty. \end{aligned} \tag{42}$$

This implies that there is no minimizer of the minimization problem (31) when $|\Omega| > \gamma^{xy}$ in 2D.

Similarly, in 3D, the argument proceeds with the central vortex line state with winding number m of the GPE (8) with $d=3$, $\beta_d=0$ and $\Omega=0$

$$\begin{aligned}
&\phi_m(\mathbf{x}) = \phi_m(r,\theta,z) = \phi_m(r,z)\, e^{im\theta}, \\
&\phi_m(r,z) = \frac{\gamma_r^{(|m|+1)/2}\gamma_z^{1/4}}{\pi^{3/4}\sqrt{|m|!}} r^{|m|} e^{-\frac{\gamma_r r^2+\gamma_z z^2}{2}},
\end{aligned} \tag{43}$$

and we conclude that there is no minimizer of the minimization problem (31) when $|\Omega| > \gamma^{xy}$ in 3D.

Remark 1. When $\gamma_{xy} < |\Omega| \le \gamma^{xy}$ in an anisotropic trap, although no rigorous mathematical justification, the numerical results in [20] show that there is no ground state of the energy functional $E_{\beta,\Omega}(\phi)$.

3.3 Stationary states as minimizer/saddle points in the linear case

For the stationary states of (13), we have the following lemma, valid in the linear case $\beta_d = 0$:

Lemma 2. *Suppose $\beta_d = 0$, $|\Omega| < \gamma_{xy}$ and $V_d(\mathbf{x}) \ge 0$ for $\mathbf{x} \in \mathbb{R}^d$, we have*
(i). The ground state ϕ^g is a global minimizer of $E_{0,\Omega}(\phi)$ over S.
(ii). Any excited state ϕ^e is a saddle point of $E_{0,\Omega}(\phi)$ over S.

Proof: Let ϕ_e be an eigenfunction of the eigenvalue problem (13) and (14). The corresponding eigenvalue is μ_e. For any function ϕ such that $E_{0,\Omega}(\phi) < \infty$ and $\|\phi_e + \phi\| = 1$, notice (14), we have that

$$\begin{aligned}
\|\phi\|^2 &= \|\phi+\phi_e\|^2 - \|\phi_e\|^2 - \int_{\mathbb{R}^d} \left(\phi^*\phi_e + \phi\phi_e^*\right)\, d\mathbf{x} \\
&= -\int_{\mathbb{R}^d} \left(\phi^*\phi_e + \phi\phi_e^*\right)\, d\mathbf{x}.
\end{aligned} \tag{44}$$

From (11) with $\psi = \phi_e + \phi$, notice (14) and (44), integration by parts, we get

$$\begin{aligned}
&E_{0,\Omega}(\phi_e+\phi) \\
&= \int_{\mathbb{R}^d} \left[\frac{1}{2}|\nabla\phi_e + \nabla\phi|^2 + V_d(\mathbf{x})|\phi_e+\phi|^2 - \Omega(\phi_e+\phi)^* L_z(\phi_e+\phi)\right]\, d\mathbf{x} \\
&= \int_{\mathbb{R}^d} \left(\frac{1}{2}|\nabla\phi_e|^2 + V_d(\mathbf{x})|\phi_e|^2 - \Omega\phi_e^* L_z\phi_e\right) d\mathbf{x} \\
&\quad + \int_{\mathbb{R}^d} \left(\frac{1}{2}|\nabla\phi|^2 + V_d(\mathbf{x})|\phi|^2 - \Omega\phi^* L_z\phi\right)\, d\mathbf{x} \\
&\quad + \int_{\mathbb{R}^d} \left(-\frac{1}{2}\Delta\phi_e + V_d(\mathbf{x})\phi_e - \Omega L_z\phi_e\right)^* \phi\, d\mathbf{x}
\end{aligned}$$

$$
\begin{aligned}
&+\int_{\mathbb{R}^d}\left(-\frac{1}{2}\Delta\phi_e+V_d(\mathbf{x})\phi_e-\Omega L_z\phi_e\right)\phi^*\,d\mathbf{x}\\
&=E_{0,\Omega}(\phi_e)+E_{0,\Omega}(\phi)-\mu_e\|\phi\|^2\\
&=E_{0,\Omega}(\phi_e)+\left[E_{0,\Omega}(\phi/\|\phi\|)-\mu_e\right]\|\phi\|^2. \qquad (45)
\end{aligned}
$$

(i) Taking $\phi_e=\phi_g$ and $\mu_e=\mu_g$ in (45) and noticing $E_{0,\Omega}(\phi/\|\phi\|)\ge E_{0,\Omega}(\phi_g)=\mu_g$ for any $\phi\neq 0$, we get immediately that ϕ_g is a global minimizer of $E_{0,\Omega}$ over S.

(ii). Taking $\phi_e=\phi_j$ and $\mu_e=\mu_j$ in (45), since $E_{0,\Omega}(\phi_g)<E_{0,\Omega}(\phi_j)$ and it is easy to find an eigenfunction ϕ of (13) such that $E_{0,\Omega}(\phi)>E_{0,\Omega}(\phi_j)$, we get immediately that ϕ_j is a saddle point of the functional $E_{0,\Omega}(\phi)$ over S.

3.4 Approximate ground state

When $\beta_d=0$ and $\Omega=0$, the ground state solution is given explicitly [18]

$$
\begin{aligned}
&\mu_{0,0}^g=\frac{1}{2}\begin{cases}\gamma_x+\gamma_y, & d=2,\\ \gamma_x+\gamma_y+\gamma_z, & d=3,\end{cases}\\
&\phi_{0,0}^g(\mathbf{x})=\frac{1}{\pi^{d/4}}\begin{cases}(\gamma_x\gamma_y)^{1/4}e^{-\frac{\gamma_x x^2+\gamma_y y^2}{2}}, & d=2,\\ (\gamma_x\gamma_y\gamma_z)^{1/4}e^{-\frac{\gamma_x x^2+\gamma_y y^2+\gamma_z z^2}{2}}, & d=3.\end{cases} \qquad (46)
\end{aligned}
$$

In fact, this solution can be viewed as an approximation of the ground state for a weakly interacting slowly rotating condensate, i.e. $|\beta_d|\ll 1$ and $|\Omega|\approx 0$.

For a condensate with strong repulsive interaction, i.e. $\beta_d\gg 1$, $|\Omega|\approx 0$, $\gamma_x=O(1)$, $\gamma_y=O(1)$ and $\gamma_z=O(1)$, the ground state can be approximated by the TF approximation in this regime [12, 18, 3, 21]:

$$
\phi_\beta^{\mathrm{TF}}(\mathbf{x})=\begin{cases}\sqrt{(\mu_\beta^{\mathrm{TF}}-V_d(\mathbf{x}))/\beta_d}, & V_d(\mathbf{x})<\mu_\beta^{\mathrm{TF}},\\ 0, & \text{otherwise},\end{cases} \qquad (47)
$$

$$
\mu_\beta^{\mathrm{TF}}=\frac{1}{2}\begin{cases}(4\beta_2\gamma_x\gamma_y/\pi)^{1/2} & d=2,\\ (15\beta_3\gamma_x\gamma_y\gamma_z/4\pi)^{2/5} & d=3.\end{cases} \qquad (48)
$$

Clearly ϕ_β^{TF} is not differentiable at $V_d(\mathbf{x})=\mu_\beta^{\mathrm{TF}}$, thus $E_{\beta,\Omega}(\phi_\beta^{\mathrm{TF}})=\infty$ and $\mu_{\beta,\Omega}(\phi_\beta^{\mathrm{TF}})=\infty$ [12, 21]. This shows that one **can't** use (11) to define the energy of the TF approximation (47). How to define the energy of the TF approximation is not clear in the literature. Using (15), (48) and (47), following [21] for non-rotating BEC, here we use the way to define the energy of the TF approximation (47) [21]:

$$
E_{\beta,\Omega}^{\mathrm{TF}}=\mu_{\beta,\Omega}^{\mathrm{TF}}-\int_{\mathbb{R}^d}\frac{\beta_d}{2}|\phi_\beta^{\mathrm{TF}}(\mathbf{x})|^4\,d\mathbf{x}=\frac{d+2}{d+4}\,\mu_\beta^{\mathrm{TF}}, \qquad d=2,3. \qquad (49)
$$

The numerical results in [20] show that the TF approximation (47) is very accurate for the density of the ground state, except at the vortex core, when $\beta_d\gg 1$ and $|\Omega|<\gamma_{xy}$, and (48) and (49) converge to the chemical potential and energy respectively only when $|\Omega|\approx 0$, but diverge when $|\Omega|$ is near γ_{xy}.

3.5 Critical angular velocity in symmetric trap

In 2D with radial symmetry and in 3D with cylindrical symmetry, for any $\beta_d \geq 0$, when $\Omega = 0$, the ground state satisfies $\phi^g_{\beta,0}(\mathbf{x}) = \phi^0_{\beta,0}(r)$ in 2D and $\phi^g_{\beta,0}(\mathbf{x}) = \phi^0_{\beta,0}(r,z)$ in 3D with $\phi^0_{\beta,0}(r)$ and $\phi^0_{\beta,0}(r,z)$ the symmetric state of the problem (13)-(14) in 2D and 3D respectively, i.e. the ground state is radially symmetric. When Ω increases to a critical angular velocity, Ω^c_β, defined as

$$\Omega^c := \Omega^c_\beta = \max\left\{\Omega \mid E_{\beta,\Omega}(\phi^g_{\beta,\Omega}) = E_{\beta,\Omega}(\phi^0_{\beta,\Omega}) = E_{\beta,0}(\phi^0_{\beta,0})\right\},$$

the energy of the ground state will be less than that of the symmetric state, i.e. symmetry breaking occurs in the ground state [67, 68]. Ω^c_β is also called as critical angular velocity for symmetry breaking in the ground state.

From the discussions and numerical results in the literatures [20, 3], we have

$$\Omega^c_0 = \gamma_r := \gamma_x = \gamma_y, \qquad 0 \leq \Omega^c_\beta < \Omega^v_\beta \leq \gamma_r, \quad \text{for } \beta_d > 0.$$

4 Numerical methods and results for ground states

In this section, we review the continuous normalized gradient flow and its backward Euler finite difference discretioznation for computing ground state of rotating BEC.

4.1 Gradient flow with discrete normalization(GFDN)

Various algorithms, e.g. imaginary time method [30, 3, 5], Sobolev gradient method [46, 45], finite element approximation [18], iterative method [29] etc., for finding the minimizer of the minimization problem (31) have been studied in the literatures. Perhaps one of the more popular technique for dealing with the normalization constraint (14) is through the splitting (or projection) scheme: (i). Apply the steepest decent method to an unconstrained minimization problem; (ii) project the solution back to the unit sphere S. This suggests us to consider gradient flow with discrete normalization (GFDN):

$$\phi_t = -\frac{\delta E_{\beta,\Omega}(\phi)}{\delta \phi^*} = \frac{1}{2}\Delta\phi - V_d(\mathbf{x})\phi - \beta_d\,|\phi|^2\phi + \Omega\, L_z\phi, \quad t_n < t < t_{n+1}, \tag{50}$$

$$\phi(\mathbf{x}, t_{n+1}) \triangleq \phi(\mathbf{x}, t^+_{n+1}) = \frac{\phi(\mathbf{x}, t^-_{n+1})}{\|\phi(\cdot, t^-_{n+1})\|}, \qquad \mathbf{x} \in \mathbb{R}^d, \quad n \geq 0, \tag{51}$$

$$\phi(\mathbf{x}, 0) = \phi_0(\mathbf{x}), \qquad \mathbf{x} \in \mathbb{R}^d \qquad \text{with} \quad \|\phi_0\| = 1; \tag{52}$$

where $0 = t_0 < t_1 < t_2 < \cdots < t_n < \cdots$ with $\Delta t_n = t_{n+1} - t_n > 0$ and $k = \max_{n\geq 0}\ \Delta t_n$, and $\phi(\mathbf{x}, t^\pm_n) = \lim_{t\to t^\pm_n} \phi(\mathbf{x}, t)$. In fact, the gradient flow

(50) can be viewed as applying the steepest descent method to the energy functional $E_{\beta,\Omega}(\phi)$ without constraint and (51) then projects the solution back to the unit sphere in order to satisfy the constraint (14). From the numerical point of view, the gradient flow (50) can be solved via traditional techniques and the normalization of the gradient flow is simply achieved by a projection at the end of each time step.

Let

$$\tilde{\phi}(\cdot,t) = \frac{\phi(\cdot,t)}{\|\phi(\cdot,t)\|}, \qquad t_n \le t \le t_{n+1}, \qquad n \ge 0. \tag{53}$$

For the gradient flow (50), it is easy to establish the following basic facts [20]:

Lemma 3. *Suppose* $V_d(\mathbf{x}) \ge 0$ *for all* $\mathbf{x} \in \mathbb{R}^d$, $\beta_d \ge 0$ *and* $\|\phi_0\| = 1$, *then*

(i). $\|\phi(\cdot,t)\| \le \|\phi(\cdot,t_n)\| = 1$ *for* $t_n \le t < t_{n+1}$, $n \ge 0$.

(ii). For any $\beta_d \ge 0$, *and all* t', t *with* $t_n \le t' < t < t_{n+1}$:

$$E_{\beta,\Omega}(\phi(\cdot,t)) \le E_{\beta,\Omega}(\phi(\cdot,t')), \qquad n \ge 0. \tag{54}$$

(iii). For $\beta_d = 0$,

$$E_{0,\Omega}(\tilde{\phi}(\cdot,t)) \le E_{0,\Omega}(\tilde{\phi}(\cdot,t_n)), \qquad t_n \le t \le t_{n+1}, \qquad n \ge 0. \tag{55}$$

From Lemma 3, we get immediately [20]

Theorem 2. *Suppose* $V_d(\mathbf{x}) \ge 0$ *for all* $\mathbf{x} \in \mathbb{R}^d$ *and* $\|\phi_0\| = 1$. *For* $\beta_d = 0$, *GFDN (50)-(52) is energy diminishing for any time step* k *and initial data* ϕ_0, *i.e.*

$$E_{0,\Omega}(\phi(\cdot,t_{n+1})) \le E_{0,\Omega}(\phi(\cdot,t_n)) \le \cdots \le E_{0,\Omega}(\phi(\cdot,0)) = E_{0,\Omega}(\phi_0), \ n \ge 0. \tag{56}$$

4.2 Continuous normalized gradient flow (CNGF)

In fact, the normalized step (51) is equivalent to solve the following ODE *exactly*

$$\phi_t(\mathbf{x},t) = \mu_\phi(t,k)\phi(\mathbf{x},t), \qquad \mathbf{x} \in \mathbb{R}^d, \quad t_n < t < t_{n+1}, \quad n \ge 0, \tag{57}$$

$$\phi(\mathbf{x},t_n^+) = \phi(\mathbf{x},t_{n+1}^-), \qquad \mathbf{x} \in \mathbb{R}^d; \tag{58}$$

where

$$\mu_\phi(t,k) \equiv \mu_\phi(t_{n+1},\Delta t_n) = -\frac{1}{2\,\Delta t_n} \ln \|\phi(\cdot,t_{n+1}^-)\|^2, \qquad t_n \le t \le t_{n+1}. \tag{59}$$

Thus the GFDN (50)-(52) can be viewed as a first-order splitting method for the gradient flow with discontinuous coefficients:

$$\phi_t = \frac{1}{2}\Delta\phi - V_d(\mathbf{x})\phi - \beta\,|\phi|^2\phi + \Omega L_z\phi + \mu_\phi(t,k)\phi, \quad \mathbf{x}\in\mathbb{R}^d, \quad t\ge 0, \tag{60}$$

$$\phi(\mathbf{x},0) = \phi_0(\mathbf{x}), \qquad \mathbf{x}\in\mathbb{R}^d \qquad \text{with} \quad \|\phi_0\| = 1. \tag{61}$$

Letting $k\to 0$ and noticing that $\phi(\mathbf{x}, t_{n+1})$ on the right hand side of (58) is the solution of (50) at $t_{n+1} = t + \Delta t_n$, we obtain

$$\begin{aligned}
\mu_\phi(t) &:= \lim_{k\to 0^+}\mu_\phi(t,k) = \lim_{\Delta t_n\to 0^+}\frac{1}{-2\ \Delta t_n}\ln\|\phi(\cdot, t_{n+1}^-)\|^2 \\
&= \lim_{\Delta t_n\to 0^+}\frac{1}{-2\ \Delta t_n}\ln\|\phi(\cdot,(t+\Delta t_n)^-)\|^2 \\
&= \lim_{\Delta t_n\to 0^+}\frac{\frac{d}{d\tau}\|\phi(\cdot,t+\tau)\|^2\big|_{\tau=\Delta t_n}}{-2\|\phi(\cdot,t+\Delta t_n)\|^2} \\
&= \lim_{\Delta t_n\to 0^+}\frac{\mu_{\beta,\Omega}(\phi(\cdot,t+\Delta t_n)}{\|\phi(\cdot,t+\Delta t_n)\|^2} = \frac{\mu_{\beta,\Omega}(\phi(\cdot,t))}{\|\phi(\cdot,t)\|^2}.
\end{aligned} \tag{62}$$

This suggests us to consider the following CNGF:

$$\phi_t = \frac{1}{2}\Delta\phi - V_d(\mathbf{x})\phi - \beta_d\,|\phi|^2\phi + \Omega L_z\phi + \mu_\phi(t)\phi,\ \ \mathbf{x}\in\mathbb{R}^d,\ \ t\ge 0, \tag{63}$$

$$\phi(\mathbf{x},0) = \phi_0(\mathbf{x}), \qquad \mathbf{x}\in\mathbb{R}^d \qquad \text{with} \quad \|\phi_0\| = 1. \tag{64}$$

In fact, the right hand side of (63) is the same as (13) if we view $\mu_\phi(t)$ as a Lagrange multiplier for the constraint (14). Furthermore for the above CNGF, as observed in [9] for non-rotating BEC, the solution of (63) also satisfies the following theorem [20]:

Theorem 3. *Suppose $V_d(\mathbf{x})\ge 0$ for all $\mathbf{x}\in\mathbb{R}^d$, $\beta_d\ge 0$ and $\|\phi_0\| = 1$. Then the CNGF (63)-(64) is normalization conserving and energy diminishing, i.e.*

$$\|\phi(\cdot,t)\|^2 = \int_{\mathbb{R}^d}|\phi(\mathbf{x},t)|^2\,d\mathbf{x} = \|\phi_0\|^2 = 1, \qquad t\ge 0, \tag{65}$$

$$\frac{d}{dt}E_{\beta,\Omega}(\phi) = -2\,\|\phi_t(\cdot,t)\|^2 \le 0\ , \qquad t\ge 0, \tag{66}$$

which in turn implies

$$E_{\beta,\Omega}(\phi(\cdot,t_1)) \ge E_{\beta,\Omega}(\phi(\cdot,t_2)), \qquad 0\le t_1\le t_2 < \infty.$$

4.3 Fully numerical discretization

We now present a numerical method to discretize the GFDN (50)-(52) (or a full discretization of CNGF (63)-(64)). For simplicity of notation we introduce the method for the case of 2D over a rectangle $\Omega_{\mathbf{x}} = [a,b]\times[c,d]$ with homogeneous Dirichlet boundary conditions. Generalizations to 3D are straightforward for tensor product grids and the results remain valid without modifications.

We choose the spatial mesh sizes $h_x = \Delta x > 0$, $h_y = \Delta y > 0$ with $h_x = (b-a)/M$, $h_y = (d-c)/N$ and M, N even positive integers, the time step is given by $k = \Delta t > 0$ and define grid points and time steps by

$$x_j := a + j\, h_x, \qquad j = 0, 1, \cdots, M, \qquad y_l = c + l\, h_y, \qquad l = 0, 1, \cdots, N,$$
$$t_n := n\, k, \qquad n = 0, 1, 2, \cdots$$

Let $\phi^n_{j,l}$ be the numerical approximation of $\phi(x_j, y_l, t_n)$ and ϕ^n the solution vector at time $t = t_n = nk$ with components $\phi^n_{j,l}$.

We use backward Euler for time discretization and second-order centered finite difference for spatial derivatives. The detail scheme is:

$$\begin{aligned}
\frac{\tilde\phi_{j,l} - \phi^n_{j,l}}{k} &= \frac{1}{2h_x^2}\left[\tilde\phi_{j+1,l} - 2\tilde\phi_{j,l} + \tilde\phi_{j-1,l}\right] + \frac{1}{2h_y^2}\left[\tilde\phi_{j,l+1} - 2\tilde\phi_{j,l} + \tilde\phi_{j,l-1}\right] \\
&\quad - V_2(x_j, y_l)\tilde\phi_{j,l} - \beta_2 \left|\phi^n_{j,l}\right|^2 \tilde\phi_{j,l} + i\Omega y_l \frac{\tilde\phi_{j+1,l} - \tilde\phi_{j-1,l}}{2h_x} \\
&\quad - i\Omega x_j \frac{\tilde\phi_{j,l+1} - \tilde\phi_{j,l-1}}{2h_y}, \qquad j = 1, \cdots, M-1, \quad l = 1, \cdots, N-1, \\
\tilde\phi_{0,l} &= \tilde\phi_{M,l} = \tilde\phi_{j,0} = \tilde\phi_{j,N} = 0, \qquad j = 0, \cdots, M, \quad l = 0, \cdots, N, \\
\phi^{n+1}_{j,l} &= \frac{\tilde\phi_{j,l}}{\|\tilde\phi\|}, \quad j = 0, 1, \cdots, M,\ l = 0, \cdots, N, \quad n = 0, 1, \cdots, \\
\phi^0_{j,l} &= \phi_0(x_j, y_l), \qquad j = 0, 1, \cdots, M; \quad l = 0, \cdots, N,
\end{aligned} \tag{67}$$

where the norm is defined as $\|\tilde\phi\|^2 = h_x h_y \sum_{j=1}^{M-1}\sum_{l=1}^{N-1} |\tilde\phi_{j,l}|^2$.

4.4 Numerical results

Many numerical results were reported in [20] for ground and central vortex states of rotating BEC in 2D and 3D. Here we only present some ground state solutions in 2D of rotating BEC for completeness. We take $d = 2$ and $\gamma_x = \gamma_y = 1$ in (8). Figures 1 and 2 plot surface and contour of the ground state $\phi^g(x, y) := \phi^g_{\beta,\Omega}(x, y)$ with $\beta_2 = 100$ for different Ω, respectively.

5 Dynamics of a rotating BEC

In this section, we provide some analytical results on the conservation of the angular momentum expectation in a symmetric trap, i.e. $\gamma_x = \gamma_y$ in (8), derive a second-order ODE for time-evolution of the condensate width, and then present some dynamic laws of a stationary state with a shifted center in a rotating BEC.

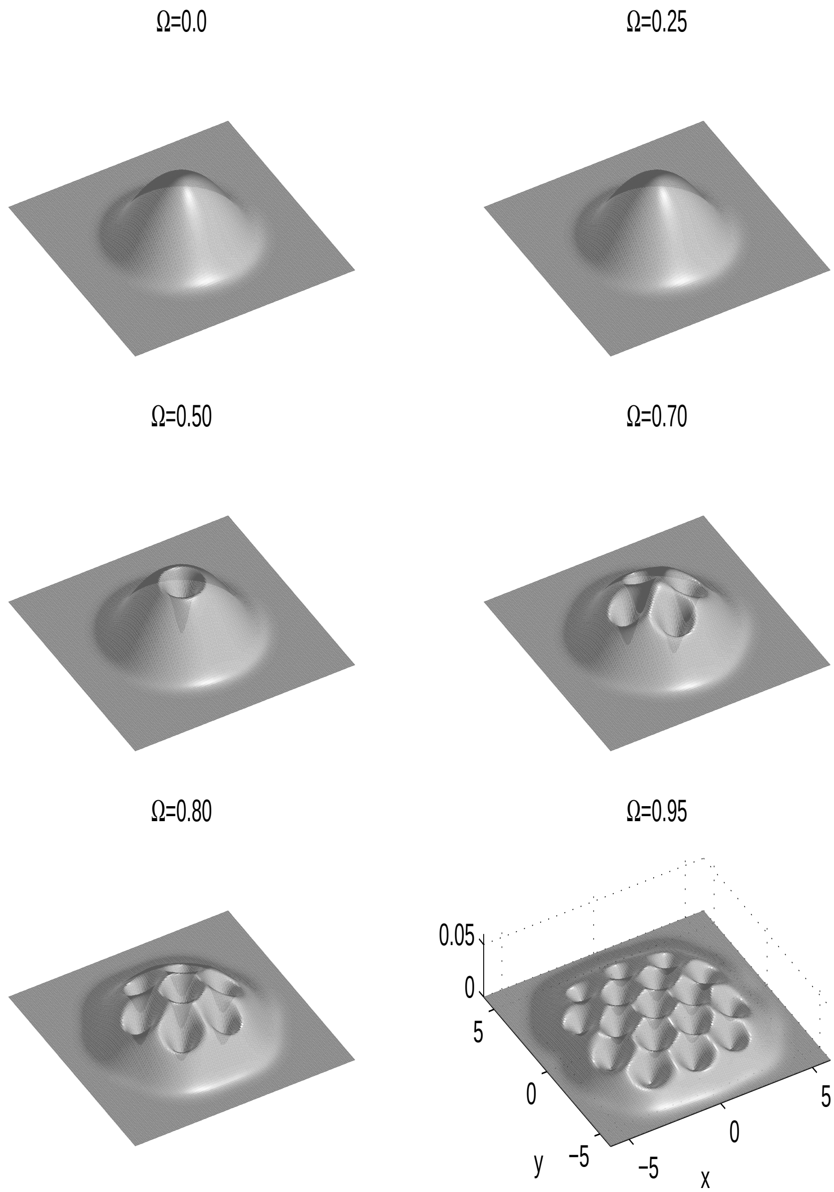

Fig. 1. Surface plots of ground state density function $|\phi^g(x,y)|^2$ in 2D with $\gamma_x = \gamma_y = 1$ and $\beta_2 = 100$ for different Ω.

5.1 Dynamics of angular momentum expectation and condensate width

As a measure of the vortex flux, we define the angular momentum expectation:

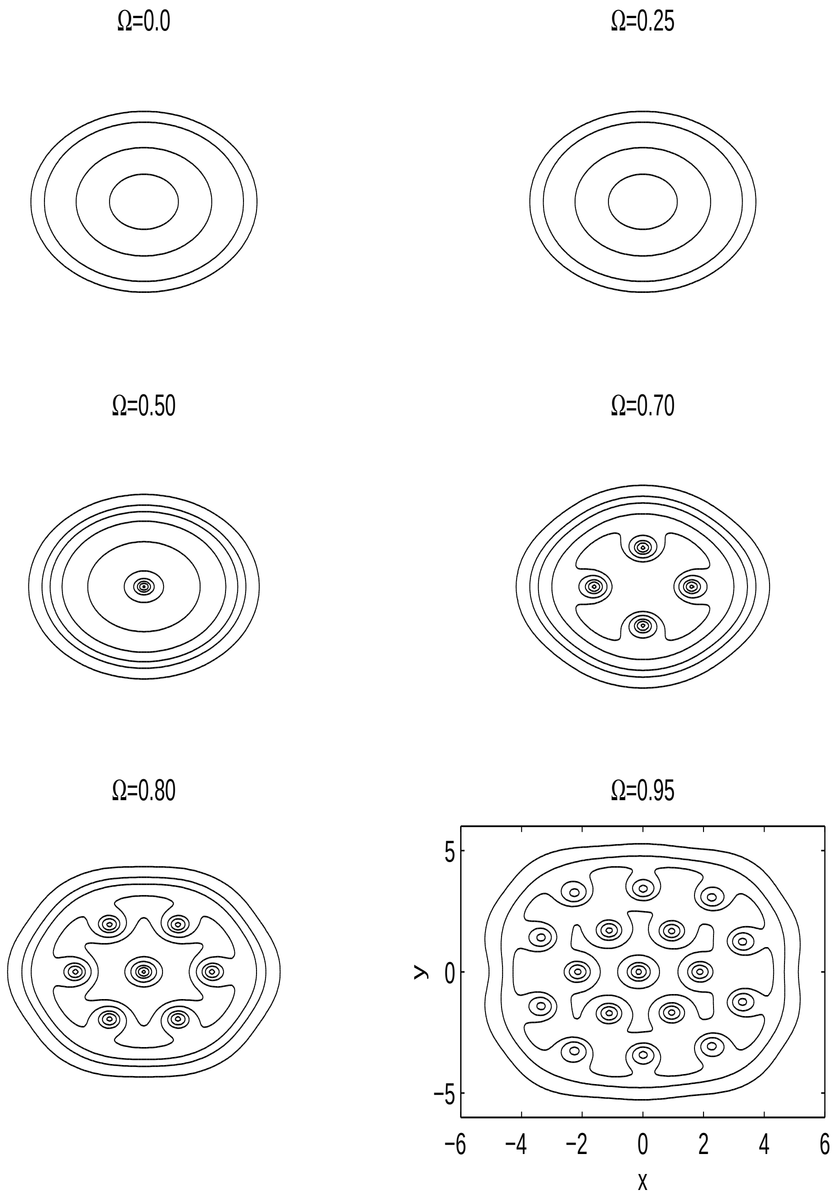

Fig. 2. Contour plots of ground state density function $|\phi^g(x,y)|^2$ in 2D with $\gamma_x = \gamma_y = 1$ and $\beta_2 = 100$ for different Ω.

$$\langle L_z\rangle(t) := \int_{\mathbb{R}^d} \psi^*(\mathbf{x},t) L_z \psi(\mathbf{x},t)\, d\mathbf{x} = i\int_{\mathbb{R}^d} \psi^*(\mathbf{x},t)(y\partial_x - x\partial_y)\psi(\mathbf{x},t) d\mathbf{x}, \tag{68}$$

for any $t \geq 0$. For the dynamics of angular momentum expectation in rotating BEC, we have the following lemma [10]:

Lemma 4. *Suppose $\psi(\mathbf{x},t)$ is the solution of the problem (8)-(9), then we have*

$$\frac{d\langle L_z\rangle(t)}{dt} = \left(\gamma_x^2 - \gamma_y^2\right)\delta_{xy}(t), \ \textit{where} \ \delta_{xy}(t) = \int_{\mathbb{R}^d} xy|\psi(\mathbf{x},t)|^2 d\mathbf{x}, \ t \geq 0 \ . \tag{69}$$

Consequently, the angular momentum expectation and energy for non-rotating part are conserved, that is, for any given initial data $\psi_0(\mathbf{x})$ in (9),

$$\langle L_z\rangle(t) \equiv \langle L_z\rangle(0), \quad E_{\beta,0}(\psi) \equiv E_{\beta,0}(\psi_0), \qquad t \geq 0 \tag{70}$$

at least for radially symmetric trap in 2D or cylindrically symmetric trap in 3D, i.e. $\gamma_x = \gamma_y$.

Another quantity characterizing the dynamics of rotating BEC is the condensate width defined as

$$\sigma_\alpha(t) = \sqrt{\delta_\alpha(t)}, \quad \text{where} \ \ \delta_\alpha(t) = \langle\alpha^2\rangle(t) = \int_{\mathbb{R}^d} \alpha^2|\psi(\mathbf{x},t)|^2 d\mathbf{x}, \tag{71}$$

for $t \geq 0$ and α being either x, y or z. For the dynamics of condensate widths, we have the following lemmas [10]:

Lemma 5. *Suppose $\psi(\mathbf{x},t)$ is the solution of problem (8)-(9), then we have*

$$\begin{aligned}\frac{d^2\delta_\alpha(t)}{dt^2} = \int_{\mathbb{R}^d}\Big[&(\partial_y\alpha - \partial_x\alpha)\left(4i\Omega\psi^*(x\partial_y + y\partial_x)\psi + 2\Omega^2(x^2-y^2)|\psi|^2\right) \\ &+2|\partial_\alpha\psi|^2 + \beta_d|\psi|^4 - 2\alpha|\psi|^2\partial_\alpha(V_d(\mathbf{x}))\Big]d\mathbf{x}, \quad t \geq 0,\end{aligned} \tag{72}$$

$$\delta_\alpha(0) = \delta_\alpha^{(0)} = \int_{\mathbb{R}^d} \alpha^2|\psi_0(\mathbf{x})|^2 d\mathbf{x}, \qquad \alpha = x, y, z, \tag{73}$$

$$\dot{\delta}_\alpha(0) = \delta_\alpha^{(1)} = 2\int_{\mathbb{R}^d} \alpha\left[-\Omega|\psi_0|^2\left(x\partial_y - y\partial_x\right)\alpha + \mathrm{Im}\left(\psi_0^*\partial_\alpha\psi_0\right)\right] \, d\mathbf{x}, \tag{74}$$

where $\mathrm{Im}(f)$ *denotes the imaginary part of f.*

From Lemma 5, we have [10]

Lemma 6. *(i) In 2D with a radial symmetric trap, i.e. $d = 2$ and $\gamma_x = \gamma_y := \gamma_r$ in (8), for any initial data $\psi_0 = \psi_0(x,y)$, we have for any $t \geq 0$,*

$$\delta_r(t) = \frac{E_{\beta,\Omega}(\psi_0) + \Omega\langle L_z\rangle(0)}{\gamma_r^2}\left[1 - \cos(2\gamma_r t)\right] + \delta_r^{(0)}\cos(2\gamma_r t) + \frac{\delta_r^{(1)}}{2\gamma_r}\sin(2\gamma_r t), \tag{75}$$

where $\delta_r(t) = \delta_x(t) + \delta_y(t)$*,* $\delta_r^{(0)} := \delta_x(0) + \delta_y(0)$*, and* $\delta_r^{(1)} := \dot{\delta}_x(0) + \dot{\delta}_y(0)$*. Furthermore, when the initial condition* $\psi_0(x,y)$ *in (9) satisfies*

$$\psi_0(x,y) = f(r)e^{im\theta} \quad \text{with} \quad m \in \mathbb{Z} \quad \text{and} \quad f(0) = 0 \quad \text{when} \quad m \neq 0, \tag{76}$$

we have, for any $t \geq 0$*,*

$$\begin{aligned}\delta_x(t) = \delta_y(t) &= \frac{1}{2}\delta_r(t) \\ &= \frac{E_{\beta,\Omega}(\psi_0) + m\Omega}{2\gamma_x^2}\left[1 - \cos(2\gamma_x t)\right] + \delta_x^{(0)} \cos(2\gamma_x t) + \frac{\delta_x^{(1)}}{2\gamma_x} \sin(2\gamma_x t). \end{aligned} \tag{77}$$

This and (71) imply that

$$\sigma_x = \sigma_y = \sqrt{\frac{E_{\beta,\Omega}(\psi_0) + m\Omega}{2\gamma_x^2}\left[1 - \cos(2\gamma_x t)\right] + \delta_x^{(0)} \cos(2\gamma_x t) + \frac{\delta_x^{(1)}}{2\gamma_x} \sin(2\gamma_x t)}. \tag{78}$$

Thus in this case, the condensate widths $\sigma_x(t)$ *and* $\sigma_y(t)$ *are periodic functions with frequency doubling the trapping frequency.*

(ii) For all other cases, we have, for any $t \geq 0$

$$\delta_\alpha(t) = \frac{E_{\beta,\Omega}(\psi_0)}{\gamma_\alpha^2} + \left(\delta_\alpha^{(0)} - \frac{E_{\beta,\Omega}(\psi_0)}{\gamma_\alpha^2}\right) \cos(2\gamma_\alpha t) + \frac{\delta_\alpha^{(1)}}{2\gamma_\alpha} \sin(2\gamma_\alpha t) + f_\alpha(t), \tag{79}$$

where $f_\alpha(t)$ *is the solution of the following second-order ODE:*

$$\frac{d^2 f_\alpha(t)}{dt^2} + 4\gamma_\alpha^2\, f_\alpha(t) = F_\alpha(t), \qquad f_\alpha(0) = \frac{df_\alpha(0)}{dt} = 0, \tag{80}$$

with

$$\begin{aligned}F_\alpha(t) = \int_{\mathbb{R}^d} \Big[& 2|\partial_\alpha \psi|^2 - 2|\nabla\psi|^2 - \beta_d|\psi|^4 + \left(2\gamma_\alpha^2\alpha^2 - 4V_d(\mathbf{x})\right)|\psi|^2 + 4\Omega\psi^* L_z\psi \\ & + (\partial_y\alpha - \partial_x\alpha)\left(4i\Omega\psi^*\left(x\partial_y + y\partial_x\right)\psi + 2\Omega^2(x^2 - y^2)|\psi|^2\right)\Big] d\mathbf{x}.\end{aligned}$$

5.2 Dynamics of a stationary state with its center shifted

Let $\phi_e(\mathbf{x})$ be a stationary state of the GPE (8) with a chemical potential μ_e [20], i.e. (μ_e, ϕ_e) satisfying

$$\mu_e\phi_e(\mathbf{x}) = -\frac{1}{2}\Delta\phi_e + V_d(\mathbf{x})\phi_e + \beta_d|\phi_e|^2\phi_e - \Omega L_z\phi_e, \qquad \|\phi_e\|^2 = 1. \tag{81}$$

If the initial data $\psi_0(\mathbf{x})$ in (9) is chosen as a stationary state with a shift in its center, one can construct an exact solution of the GPE (8) with a harmonic oscillator potential. This kind of analytical construction can be used, in particular, in the benchmark and validation of numerical algorithms for GPE. In [40], a similar kind of solution was constructed for GPE and a second order ODE system was derived for the dynamics of the center, but the results there were valid only for non-rotating BEC, i.e. $\Omega = 0$. Modifications must be made for the rotating BEC, i.e. $\Omega \neq 0$. Later, in [22], similar results were extended to the case of a general Hamiltonian but without specifying the initial data for the ODE system. Here we present the dynamic laws for the rotating BEC [10]:

Lemma 7. *If the initial data* $\psi_0(\mathbf{x})$ *in (9) is chosen as*

$$\psi_0(\mathbf{x}) = \phi_e(\mathbf{x} - \mathbf{x}_0), \qquad \mathbf{x} \in \mathbb{R}^d, \tag{82}$$

where $\mathbf{x}_0$ *is a given point in* $\mathbb{R}^d$*, then the exact solution of (8)-(9) satisfies:*

$$\psi(\mathbf{x}, t) = \phi_e(\mathbf{x} - \mathbf{x}(t))\, e^{-i\mu_e t}\, e^{iw(\mathbf{x},t)}, \qquad \mathbf{x} \in \mathbb{R}^d, \quad t \geq 0, \tag{83}$$

where for any time $t \geq 0$*,* $w(\mathbf{x}, t)$ *is linear for* $\mathbf{x}$*, i.e.*

$$w(\mathbf{x}, t) = \mathbf{c}(t) \cdot \mathbf{x} + g(t), \quad \mathbf{c}(t) = (c_1(t), \cdots, c_d(t))^T, \quad \mathbf{x} \in \mathbb{R}^d,\ t \geq 0, \tag{84}$$

and $\mathbf{x}(t)$ *satisfies the following second-order ODE system:*

$$\ddot{x}(t) - 2\Omega\dot{y}(t) + \left(\gamma_x^2 - \Omega^2\right) x(t) = 0, \tag{85}$$

$$\ddot{y}(t) + 2\Omega\dot{x}(t) + \left(\gamma_y^2 - \Omega^2\right) y(t) = 0, \qquad t \geq 0, \tag{86}$$

$$x(0) = x_0, \quad y(0) = y_0, \qquad \dot{x}(0) = \Omega y_0, \qquad \dot{y}(0) = -\Omega x_0\ . \tag{87}$$

Moreover, if in 3D, another ODE needs to be added:

$$\ddot{z}(t) + \gamma_z^2 z(t) = 0, \qquad z(0) = z_0, \qquad \dot{z}(0) = 0. \tag{88}$$

5.3 Analytical solutions for the center of mass

Without loss of generality, in this subsection, we assume $\gamma_x = 1$ and $\gamma_x \leq \gamma_y$ in (85)-(88). From (81) and (83), changing of variables, we get

$$\begin{aligned}\langle \mathbf{x} \rangle(t) &:= \int_{\mathbb{R}^d} \mathbf{x} |\psi(\mathbf{x}, t)|^2\, d\mathbf{x} = \int_{\mathbb{R}^d} \mathbf{x} |\phi_e(\mathbf{x} - \mathbf{x}(t))|^2\, d\mathbf{x} \\ &= \int_{\mathbb{R}^d} (\mathbf{x} + \mathbf{x}(t)) |\phi_e(\mathbf{x})|^2\, d\mathbf{x} = \mathbf{x}(t), \quad t \geq 0.\end{aligned} \tag{89}$$

This immediately implies that the dynamics of the center of mass is the same as that of $\mathbf{x}(t)$, i.e. satisfying the ODE system (85)-(88). It is easy to see that the solution of (88) is

$$z(t) = z_0 \cos(\gamma_z t), \qquad t \geq 0, \tag{90}$$

thus, $z(t)$ is a periodic function with period $T_z = 2\pi/\gamma_z$. Furthermore, when $\Omega \neq 0$, dividing both sides of (85) by 2Ω, we get

$$\dot{y}(t) = \frac{1}{2\Omega}\left(\ddot{x}(t) + \left(\gamma_x^2 - \Omega^2\right) x(t)\right), \qquad t \geq 0. \tag{91}$$

Differentiating (86) with respect to t, we obtain

$$y^{(3)}(t) + 2\Omega\ddot{x}(t) + \left(\gamma_y^2 - \Omega^2\right)\dot{y}(t) = 0, \qquad t \geq 0. \tag{92}$$

Plugging (91) into (92), we get the following fourth-order ODE for $x(t)$

$$x^{(4)}(t) + \left(\gamma_x^2 + \gamma_y^2 + 2\Omega^2\right)\ddot{x}(t) + \left(\gamma_x^2 - \Omega^2\right)\left(\gamma_y^2 - \Omega^2\right) x(t) = 0, \; t \geq 0. \tag{93}$$

The characteristic equation of (93) is

$$\lambda^4 + \left(\gamma_x^2 + \gamma_y^2 + 2\Omega^2\right)\lambda^2 + \left(\gamma_x^2 - \Omega^2\right)\left(\gamma_y^2 - \Omega^2\right) = 0. \tag{94}$$

In the following, we will discuss the solutions of the ODE system (85)-(87) in different parameter regimes of trapping frequencies and angular rotation speed Ω.

For a non-rotating BEC, i.e. $\Omega \equiv 0$ in GPE (8), the second-order ODE system (85)-(87) collapses to

$$\ddot{x}(t) + \gamma_x^2 x(t) = 0, \qquad \ddot{y}(t) + \gamma_y^2 y(t) = 0, \qquad t \geq 0, \tag{95}$$

$$x(0) = x_0, \quad y(0) = y_0, \quad \dot{x}(0) = \dot{y}(0) = 0. \tag{96}$$

It is straightforward to see that the solution of (95)-(96) is

$$x(t) = x_0\cos(\gamma_x t), \qquad y(t) = y_0\cos(\gamma_y t), \qquad t \geq 0, \tag{97}$$

which implies that both $x(t)$ and $y(t)$ are periodic functions with periods $T_x = 2\pi/\gamma_x$ and $T_y = 2\pi/\gamma_y$, respectively.

For a rotating BEC with a symmetric trap, i.e. $\Omega \neq 0$ in (8) and $\gamma_x \equiv \gamma_y$, we have the following solution for the second order ODE system (85)-(87) [77]:

Lemma 8. *When $\Omega \neq 0$ and $\gamma_x \equiv \gamma_y$ in (85)-(87), the solutions of $x(t)$ and $y(t)$ for the motion of the center are*

$$x(t) = \frac{x_0}{2}\left[\cos(at) + \cos(bt)\right] + \frac{|\Omega| y_0}{2\Omega}\left[\sin(at) - \sin(bt)\right], \tag{98}$$

$$y(t) = \frac{y_0}{2}\left[\cos(at) + \cos(bt)\right] + \frac{|\Omega| x_0}{2\Omega}\left[-\sin(at) + \sin(bt)\right], \quad t \geq 0, \tag{99}$$

where

$$a = \gamma_x + |\Omega|, \qquad b = \gamma_x - |\Omega|.$$

Furthermore, we can get the distance between the center of mass and the trap center is a periodic function with period $T = \pi/\gamma_x$, i.e.

$$|\mathbf{x}(t)| := \sqrt{x^2(t) + y^2(t)} = \sqrt{x_0^2 + y_0^2}\,|\cos(\gamma_x t)|, \qquad t \geq 0. \tag{100}$$

For a rotating BEC with an anisotropic trap, i.e. $\Omega \neq 0$ in (8) and $\gamma_x < \gamma_y$, we will present the analytical solutions in four different cases: (a). $|\Omega| = \gamma_x$; (b). $|\Omega| = \gamma_y$; (c). $0 < |\Omega| < \gamma_x$ or $|\Omega| > \gamma_y$; and (d). $\gamma_x < \Omega < \gamma_y$.

For $|\Omega| = \gamma_x$, we have [77]

Lemma 9. *When $|\Omega| = \gamma_x < \gamma_y$ in (85)-(87), the solutions of $x(t)$ and $y(t)$ for the motion of the center are*

$$x(t) = \frac{x_0}{a^2}\left[(\gamma_y^2 + \Omega^2) + 2\Omega^2\cos(at)\right] + \frac{\Omega y_0}{a^2}\left[-(\gamma_y^2 - \Omega^2)t + \frac{2(\gamma_y^2+\Omega^2)}{a}\sin(at)\right], \tag{101}$$

$$y(t) = \frac{y_0}{a^2}\left[2\Omega^2 + (\gamma_y^2 + \Omega^2)\cos(at)\right] - \frac{\Omega x_0}{a}\sin(at), \qquad t \geq 0; \tag{102}$$

where $a = \sqrt{\gamma_y^2 + 3\Omega^2}$. This implies that the center moves on an ellipse when $y_0 = 0$, and moves to infinity when $y_0 \neq 0$.

Similarly for $\gamma_x < |\Omega| = \gamma_y$, we have [77]

Lemma 10. *When $\gamma_x < \gamma_y = |\Omega|$ in (85)-(87), the solutions of $x(t)$ and $y(t)$ for the motion of the center are*

$$x(t) = \frac{x_0}{a^2}\left[2\Omega^2 + (\gamma_x^2 + \Omega^2)\cos(at)\right] + \frac{\Omega y_0}{a}\sin(at), \qquad t \geq 0, \tag{103}$$

$$y(t) = \frac{y_0}{a^2}\left[(\gamma_x^2 + \Omega^2) + 2\Omega^2\cos(at)\right] + \frac{\Omega x_0}{a^2}\left[(\gamma_x^2 - \Omega^2)t - \frac{2(\gamma_x^2+\Omega^2)}{a}\sin(at)\right], \tag{104}$$

where $a = \sqrt{\gamma_x^2 + 3\Omega^2}$. Again this implies that the center moves on an ellipse when $x_0 = 0$, and moves to infinity when $x_0 \neq 0$.

If $\Omega \neq 0$, γ_x or γ_y, let $\delta_1 = (\gamma_x^2+\gamma_y^2+2\Omega^2)/2$, $\delta_2 = \sqrt{\delta_1^2 - (\gamma_x^2 - \Omega^2)\left(\gamma_y^2 - \Omega^2\right)}$, $a = \sqrt{|\delta_1 - \delta_2|}$ and $b = \sqrt{\delta_1 + \delta_2}$. When $0 < |\Omega| < \gamma_x$ or $|\Omega| > \gamma_y$, we have $0 < \delta_2 < \delta_1$. Thus we get the four roots for the characteristic equation (94)

$$\lambda_{1,2} = \pm i\sqrt{\delta_1 - \delta_2} = \pm a\, i, \qquad \lambda_{3,4} = \pm i\sqrt{\delta_1 + \delta_2} = \pm b\, i. \tag{105}$$

Following the procedure in the proof of Lemma 2.1, after a detailed computation, we get the solution of the ODE system (85)-(87) in this case

Lemma 11. *When $\gamma_x < \gamma_y$, and $0 < |\Omega| < \gamma_x$ or $|\Omega| > \gamma_y$, we have the solution $x(t)$ and $y(t)$ of the ODE system (85)-(87)*

$$x(t) = c_1\cos(at) + c_2\sin(at) + c_3\cos(bt) + c_4\sin(bt), \tag{106}$$

$$y(t) = c_5\cos(at) + c_6\sin(at) + c_7\cos(bt) + c_8\sin(bt), \quad t \geq 0, \tag{107}$$

where

$$c_1 = \frac{\left(\gamma_x^2 + \Omega^2 - b^2\right) x_0}{a^2 - b^2}, \quad c_2 = \frac{a\Omega \left(\gamma_x^2 - \Omega^2 + b^2\right) y_0}{\left(\gamma_x^2 - \Omega^2\right)\left(a^2 - b^2\right)},$$
$$c_3 = -\frac{\left(\gamma_x^2 + \Omega^2 - a^2\right) x_0}{a^2 - b^2}, \quad c_4 = -\frac{b\Omega \left(\gamma_x^2 - \Omega^2 + a^2\right) y_0}{\left(\gamma_x^2 - \Omega^2\right)\left(a^2 - b^2\right)},$$
$$c_5 = -\frac{\left(\gamma_x^2 - \Omega^2 - a^2\right)\left(\gamma_x^2 - \Omega^2 + b^2\right) y_0}{2\left(\gamma_x^2 - \Omega^2\right)\left(a^2 - b^2\right)},$$
$$c_6 = \frac{\left(\gamma_x^2 - \Omega^2 - a^2\right)\left(\gamma_x^2 + \Omega^2 - b^2\right) x_0}{2a\Omega\left(a^2 - b^2\right)},$$
$$c_7 = \frac{\left(\gamma_x^2 - \Omega^2 + a^2\right)\left(\gamma_x^2 - \Omega^2 - b^2\right) y_0}{2\left(\gamma_x^2 - \Omega^2\right)\left(a^2 - b^2\right)},$$
$$c_8 = -\frac{\left(\gamma_x^2 - \Omega^2 - b^2\right)\left(\gamma_x^2 + \Omega^2 - a^2\right) x_0}{2b\Omega\left(a^2 - b^2\right)}.$$

This implies that the graph of the trajectory is a bounded set.

Similarly, when $\gamma_x < |\Omega| < \gamma_y$, we have $\delta_2 > \delta_1$. Thus we get the four roots for the characteristic equation (94)

$$\lambda_{1,2} = \pm\sqrt{\delta_2 - \delta_1} = \pm a, \qquad \lambda_{3,4} = \pm i\sqrt{\delta_1 + \delta_2} = \pm b\, i. \tag{108}$$

Following the procedure in the proof of Lemma 2.1, after a detailed computation, we get the solution of the ODE system (85)-(87) in this case

Lemma 12. *When $\gamma_x < |\Omega| < \gamma_y$, we have the solution $x(t)$ and $y(t)$ of the ODE system (85)-(87)*

$$x(t) = d_1 e^{at} + d_2 e^{-at} + d_3 \cos(bt) + d_4 \sin(bt), \tag{109}$$
$$y(t) = d_5 e^{at} + d_6 e^{-at} + d_7 \cos(bt) + d_8 \sin(bt), \quad t \ge 0, \tag{110}$$

where

$$d_1 = \frac{1}{2}(c_1 - c_2), \qquad d_2 = -\frac{1}{2}(c_1 + c_2), \qquad d_3 = c_3,$$
$$d_4 = c_4, \qquad d_7 = c_7, \qquad d_8 = c_8,$$
$$d_5 = \frac{\left(\gamma_x^2 - \Omega^2 + a^2\right)}{4a\Omega}(c_1 - c_2), \qquad d_6 = \frac{\left(\gamma_x^2 - \Omega^2 + a^2\right)}{4a\Omega}(c_1 + c_2),$$

with $c_1, \ldots, c_8$ constants defined in Lemma 2.4. From the above solution, we can see that if $c_1 = c_2$, i.e. $y_0 = \frac{\left(\gamma_x^2 - \Omega^2\right)\left(\gamma_x^2 + \Omega^2 - b^2\right) x_0}{a\Omega\left(\gamma_x^2 - \Omega^2 + b^2\right)}$, the graph of the trajectory is a bounded set; otherwise, the center will move to the infinity exponentially fast and satisfies

$$\lim_{t\to\infty} \frac{y(t)}{x(t)} = \frac{c_5}{c_1} = \frac{\left(\gamma_x^2 - \Omega^2 + a^2\right)}{2a\Omega}. \tag{111}$$

5.4 Dynamics of the total density in the presence of dissipation

Consider a more general GPE of the form:

$$(i-\lambda)\partial_t\psi(\mathbf{x},t) = -\frac{1}{2}\Delta\psi + V(\mathbf{x},t)\psi + \beta_d|\psi|^2\psi - \Omega L_z\psi, \;\; \mathbf{x}\in\mathbb{R}^d, \quad (112)$$

$$\psi(\mathbf{x},0) = \psi_0(\mathbf{x}), \quad \mathbf{x}\in\mathbb{R}^d; \quad (113)$$

where $\lambda \geq 0$ is a real parameter that models a dissipation mechanism [4, 10] and $V(\mathbf{x},t) = V_d(\mathbf{x}) + W(\mathbf{x},t)$ with $W(\mathbf{x},t)$ an external driven field [25, 26, 50]. Typical external driven fields used in physics literatures include a Delta kicked potential [50]

$$W(x,t) = K_s\cos(k_s x)\sum_{n=-\infty}^{\infty}\delta(t-n\tau), \quad (114)$$

with K_s being the kick strength, k_s the wavenumber, τ the time interval between kicks, and $\delta(\tau)$ the Dirac delta function; or a far-blue detuned Gaussian laser beam stirrer [10, 25, 26]

$$W(\mathbf{x},t) = W_s(t)\exp\left[-\left(\frac{|\mathbf{x}-\mathbf{x}_s(t)|^2}{w_s/2}\right)\right], \quad (115)$$

with $W_s(t)$ being the height, w_s the width and $\mathbf{x}_s(t)$ the position of the stirrer. In addition, we note that to study the onset of energy dissipation in a BEC stirred by a laser field, another possibility is to view the beam as an translating *obstacle* [4] instead of introducing the Gaussian potential.

While the total density remains constant with $\lambda = 0$, in the more general case, we have the following lemma for the dynamics of the total density [10]:

Lemma 13. *Let $\psi(\mathbf{x},t)$ be the solution of (112)- (113), then the total density satisfies*

$$\dot{N}(\psi)(t) = \frac{d}{dt}\int_{\mathbb{R}^d}|\psi(\mathbf{x},t)|^2\,d\mathbf{x} = -\frac{2\lambda}{1+\lambda^2}\mu_{\beta,\Omega}(\psi), \qquad t\geq 0, \quad (116)$$

where

$$\mu_{\beta,\Omega}(\psi) = \int_{\mathbb{R}^d}\left[\frac{1}{2}|\nabla\psi|^2 + V(\mathbf{x},t)|\psi|^2 + \beta_d|\psi|^4 - \Omega\mathrm{Re}(\psi^* L_z\psi)\right]d\mathbf{x}.$$

Consequently, the total density decreases when $\lambda > 0$ and $|\Omega| \leq \gamma_{xy} := \min\{\gamma_x,\gamma_y\}$.

6 Numerical methods for computing dynamics in rotating BEC

In this section, we review the efficient and accurate numerical methods proposed recently to solve the following GPE for dynamics of rotating BEC.

Due to the trapping potential $V_d(\mathbf{x})$, the solution $\psi(\mathbf{x},t)$ of (112)-(113) decays to zero exponentially fast when $|\mathbf{x}| \to \infty$. Thus in practical computation, we truncate the problem (112)-(113) into a bounded computational domain with the homogeneous Dirichlet boundary condition:

$$(i-\lambda)\partial_t\psi(\mathbf{x},t) = -\frac{1}{2}\Delta\psi + V(\mathbf{x},t)\psi + \beta_d|\psi|^2\psi - \Omega L_z\psi, \ \mathbf{x}\in\Omega_{\mathbf{x}}, \tag{117}$$

$$\psi(\mathbf{x},t) = 0, \qquad \mathbf{x}\in\Gamma = \partial\Omega_{\mathbf{x}}, \qquad t\ge 0, \tag{118}$$

$$\psi(\mathbf{x},0) = \psi_0(\mathbf{x}), \quad \mathbf{x}\in\bar{\Omega}_{\mathbf{x}}; \tag{119}$$

where $\Omega_{\mathbf{x}}$ is a bounded computational domain to be specified later. The use of more sophisticated radiation boundary conditions is an interesting topic that remains to be examined in the future.

6.1 Time-splitting

We choose a time step size $\Delta t > 0$. For $n = 0,1,2,\cdots$, from time $t = t_n = n\Delta t$ to $t = t_{n+1} = t_n + \Delta t$, the GPE (117) is solved in two splitting steps. One solves first

$$(i-\lambda)\ \partial_t\psi(\mathbf{x},t) = -\frac{1}{2}\Delta\psi - \Omega L_z\psi \tag{120}$$

for the time step of length Δt, followed by solving

$$(i-\lambda)\ \partial_t\psi(\mathbf{x},t) = V(\mathbf{x},t)\psi + \beta_d|\psi|^2\psi, \tag{121}$$

for the same time step. Equation (120) will be discretized in detail in the next two subsections. For $t\in[t_n,t_{n+1}]$, after dividing (121) by $(i-\lambda)$, multiplying it by ψ^* and adding with its complex conjugate, we obtain the following ODE for $\rho(\mathbf{x},t) = |\psi(\mathbf{x},t)|^2$:

$$\partial_t\rho(\mathbf{x},t) = -\frac{2\lambda}{1+\lambda^2}\left[V(\mathbf{x},t)\rho(\mathbf{x},t) + \beta_d\rho^2(\mathbf{x},t)\right],\ \mathbf{x}\in\Omega_{\mathbf{x}},\ t_n\le t\le t_{n+1}. \tag{122}$$

The ODE for the phase angle $\phi(\mathbf{x},t)$ (determined as $\psi = \sqrt{\rho}e^{i\phi}$) is given by

$$\phi_t = -\frac{1}{1+\lambda^2}\left[V(\mathbf{x},t) + \beta_d\rho(\mathbf{x},t)\right],\ \mathbf{x}\in\Omega_{\mathbf{x}},\ t_n\le t\le t_{n+1}. \tag{123}$$

For $\lambda\ne 0$, by (122), the above is equivalent to

$$\phi_t = \frac{1}{2\lambda}\partial_t \ln\rho\ , \qquad \mathbf{x}\in\Omega_{\mathbf{x}},\ t_n\le t\le t_{n+1}. \tag{124}$$

Denote $V_n(\mathbf{x},t) = \int_{t_n}^t V(\mathbf{x},\tau)d\tau$, we can solve (122) to get,

$$\rho(\mathbf{x},t) = \frac{\rho(\mathbf{x},t_n)\ \exp[\frac{-2\lambda V_n(\mathbf{x},t)}{1+\lambda^2}]}{1+\rho(\mathbf{x},t_n)\frac{2\lambda\beta_d}{1+\lambda^2}\int_{t_n}^t \exp[\frac{-2\lambda V_n(\mathbf{x},\tau)}{1+\lambda^2}]\ d\tau}\ . \tag{125}$$

Consequently, in the special case $V(\mathbf{x},t)=V(\mathbf{x})$, we have some exact analytical solutions given by

$$\rho(\mathbf{x},t)=\begin{cases}\rho(\mathbf{x},t_n), & \lambda=0,\\[2ex] \dfrac{(1+\lambda^2)\rho(\mathbf{x},t_n)}{(1+\lambda^2)+2\lambda\beta_d(t-t_n)\rho(\mathbf{x},t_n)}, & V(\mathbf{x})=0,\\[2ex] \dfrac{V(\mathbf{x})\rho(\mathbf{x},t_n)\ \exp[\frac{-2\lambda V(\mathbf{x})(t-t_n)}{1+\lambda^2}]}{V(\mathbf{x})+\left(1-\exp[\frac{-2\lambda V(\mathbf{x})(t-t_n)}{1+\lambda^2}]\right)\beta_d\rho(\mathbf{x},t_n)}, & V(\mathbf{x})\neq 0.\end{cases} \tag{126}$$

Plugging (125) into (123), we get for $t\in[t_n,t_{n+1}]$,

$$\psi(\mathbf{x},t)=\psi(\mathbf{x},t_n)\sqrt{U_n(\mathbf{x},t)}\exp\left[-\frac{i}{1+\lambda^2}\left(V_n(\mathbf{x},t)+\beta_d\int_{t_n}^{t}\rho(\mathbf{x},\tau)d\tau\right)\right], \tag{127}$$

where

$$U_n(\mathbf{x},t)=\frac{\exp[\frac{-2\lambda V_n(\mathbf{x},t)}{1+\lambda^2}]}{1+|\psi(\mathbf{x},t_n)|^2\frac{2\lambda\beta_d}{1+\lambda^2}\int_{t_n}^{t}\exp[\frac{-2\lambda V_n(\mathbf{x},\tau)}{1+\lambda^2}]\,d\tau}. \tag{128}$$

Again, with $V(\mathbf{x},t)=V(\mathbf{x})$, we can integrate exactly to get

$$\psi(\mathbf{x},t)=\psi(\mathbf{x},t_n)\begin{cases}\exp\left[-i(\beta_d|\psi(\mathbf{x},t_n)|^2+V(\mathbf{x}))(t-t_n)\right], & \lambda=0,\\[2ex] \sqrt{\hat{U}_n(\mathbf{x},t)}\exp[\frac{i}{2\lambda}\ln\hat{U}_n(\mathbf{x},t)], & \lambda\neq 0;\end{cases} \tag{129}$$

where

$$\hat{U}_n(\mathbf{x},t)=\begin{cases}\dfrac{1+\lambda^2}{1+\lambda^2+2\lambda\beta_d(t-t_n)|\psi(\mathbf{x},t_n)|^2}, & V(\mathbf{x})=0,\\[2ex] \dfrac{V(\mathbf{x})\exp[-\frac{2\lambda(t-t_n)V(\mathbf{x})}{1+\lambda^2}]}{V(\mathbf{x})+\left(1-\exp[-\frac{2\lambda(t-t_n)V(\mathbf{x})}{1+\lambda^2}]\right)\beta_d|\psi(\mathbf{x},t_n)|^2}, & V(\mathbf{x})\neq 0.\end{cases}$$

Remark 2. If the function $V_n(\mathbf{x},t)$ as well as other integrals in (125), (127), and (128) can not be evaluated analytically, numerical quadrature can be used, e.g.

$$\begin{aligned}V_n(\mathbf{x},t_{n+1})&=\int_{t_n}^{t_{n+1}}V(\mathbf{x},\tau)\,d\tau\\ &\approx\frac{\Delta t}{6}\left[V(\mathbf{x},t_n)+4V(\mathbf{x},t_n+\Delta t/2)+V(\mathbf{x},t_{n+1})\right].\end{aligned}$$

6.2 Discretization by using polar/cylindrical coordinate

To solve (120), we choose $\Omega_{\mathbf{x}} = \{(x,y),\ r = \sqrt{x^2+y^2} < R\}$ in 2D, and respectively $\Omega_{\mathbf{x}} = \{(x,y,z),\ r = \sqrt{x^2+y^2} < R,\ a < z < b\}$ in 3D, with R, $|a|$ and b sufficiently large, and try to formulate the equation in a variable separable form. When $d=2$, we use the polar coordinate (r,θ), and discretize in the θ-direction by a Fourier pseudo-spectral method, in the r-direction by a finite element method (FEM) and in time by a Crank-Nicolson (C-N) scheme. Assume

$$\psi(r,\theta,t) = \sum_{l=-L/2}^{L/2-1} \widehat{\psi}_l(r,t)\ e^{il\theta}, \tag{130}$$

where L is an even positive integer and $\widehat{\psi}_l(r,t)$ is the Fourier coefficient for the l-th mode. Plugging (130) into (120), noticing the orthogonality of the Fourier functions, we obtain for $-\frac{L}{2} \le l \le \frac{L}{2}-1$ and $0 < r < R$:

$$(i-\lambda)\,\partial_t\widehat{\psi}_l(r,t) = -\frac{1}{2r}\frac{\partial}{\partial r}\left(r\frac{\partial\widehat{\psi}_l(r,t)}{\partial r}\right) + \left(\frac{l^2}{2r^2} - l\Omega\right)\widehat{\psi}_l(r,t), \tag{131}$$

$$\widehat{\psi}_l(R,t) = 0 \quad (\text{for all } l), \qquad \widehat{\psi}_l(0,t) = 0 \quad (\text{for } l \neq 0). \tag{132}$$

Let P^k denote all polynomials with degree at most k, $M > 0$ be a chosen integer, $0 = r_0 < r_1 < r_2 < \cdots < r_M = R$ be a partition for the interval $[0,R]$ with a mesh size $h = \max_{0\le m<M}\{r_{m+1} - r_m\}$. Define a FEM subspace by

$$U^h = \left\{u^h \in C[0,R]\ |\ \ u^h\big|_{[r_m,r_{m+1}]} \in P^k,\ 0 \le m < M,\ u^h(R) = 0\right\}$$

for $l = 0$, and for $l \neq 0$,

$$U^h = \left\{u^h \in C[0,R]\ |\ \ u^h\big|_{[r_m,r_{m+1}]} \in P^k,\ 0 \le m < M,\ u^h(0) = u^h(R) = 0\right\},$$

then we obtain the FEM approximation for (131)-(132): Find $\hat{\psi}_l^h = \hat{\psi}_l^h(\cdot,t) \in U^h$ such that for all $\phi^h \in U^h$ and $t_n \le t \le t_{n+1}$,

$$(i-\lambda)\,\frac{d}{dt}A(\hat{\psi}_l^h(\cdot,t),\phi^h) = B(\hat{\psi}_l^h(\cdot,t),\phi^h) + l^2C(\hat{\psi}_l^h,\phi^h) - l\Omega A(\hat{\psi}_l^h,\phi^h), \tag{133}$$

where

$$A(u^h,v^h) = \int_0^R r\ u^h(r)\ v^h(r)\ dr, \qquad B(u^h,v^h) = \int_0^R \frac{r}{2}\ \frac{du^h(r)}{dr}\ \frac{dv^h(r)}{dr}\ dr,$$
$$C(u^h,v^h) = \int_0^R \frac{1}{2r}\ u^h(r)\ v^h(r)\ dr, \qquad u^h,\ v^h \in U^h.$$

The ODE system (133) is then discretized by the standard Crank-Nicolson scheme in time. Although an implicit time discretization is applied for (133), the 1D nature of the problem makes the coefficient matrix for the linear system band-limited. For example, if the piecewise linear polynomial is used, i.e. $k = 1$ in U^h, the matrix is tridiagonal. Fast algorithms can be applied to solve the resulting linear systems.

In practice, we always use the second-order Strang splitting [71], i.e. from time $t = t_n$ to $t = t_{n+1}$: i) first evolve (121) for half time step $\Delta t/2$ with initial data given at $t = t_n$; ii) then evolve (120) for one time step Δt starting with the new data; iii) and evolve (121) for half time step $\Delta t/2$ with the newer data. Other ways to discretize (131) were also proposed in [10]. This method was demonstrated to be spectral accuracy in transverse direction, second or fourth-order accuracy in radial direction and second accuracy in time [10]

6.3 Discretization by using ADI technique

To solve (120) in another way, we choose $\Omega_{\mathbf{x}} = [a, b] \times [c, d]$ in 2D, and resp., $\Omega_{\mathbf{x}} = [a, b] \times [c, d] \times [e, f]$ in 3D, with $|a|$, b, $|c|$, d, $|e|$ and f sufficiently large. For simplicity of notation, here we assume $\lambda = 0$ and $V(\mathbf{x}, t) = V(\mathbf{x})$ in (117).

When $d = 2$ in (120), we choose mesh sizes $\Delta x > 0$ and $\Delta y > 0$ with $\Delta x = (b - a)/M$ and $\Delta y = (d - c)/N$ for M and N even positive integers, and let the grid points be

$$x_j = a + j\Delta x, \quad j = 0, 1, 2, \cdots, M; \quad y_k = c + k\Delta y, \quad k = 0, 1, 2, \cdots, N.$$

Let ψ^n_{jk} be the approximation of $\psi(x_j, y_k, t_n)$ and ψ^n be the solution vector with component ψ^n_{jk}.

From time $t = t_n$ to $t = t_{n+1}$, we solve (120) first

$$i\,\partial_t\psi(\mathbf{x}, t) = -\frac{1}{2}\partial_{xx}\psi(\mathbf{x}, t) - i\Omega y\partial_x\psi(\mathbf{x}, t), \tag{134}$$

for the time step of length Δt, followed by solving

$$i\,\partial_t\psi(\mathbf{x}, t) = -\frac{1}{2}\partial_{yy}\psi(\mathbf{x}, t) + i\Omega x\partial_y\psi(\mathbf{x}, t), \tag{135}$$

for the same time step.

For each fixed y, the operator in the equation (134) is in x-direction with constant coefficients and thus we can discretize it in x-direction by a Fourier pseudospectral method. Assume

$$\psi(x, y, t) = \sum_{p=-M/2}^{M/2-1} \widehat{\psi}_p(y, t)\ \exp[i\mu_p(x - a)], \tag{136}$$

where $\mu_p = \frac{2p\pi}{b-a}$ and $\widehat{\psi}_p(y, t)$ is the Fourier coefficient for the p-th mode in x-direction. Plugging (136) into (134), noticing the orthogonality of the Fourier functions, we obtain for $-\frac{M}{2} \le p \le \frac{M}{2} - 1$ and $c \le y \le d$:

$$i\,\partial_t \widehat{\psi}_p(y,t) = \left(\frac{1}{2}\mu_p^2 + \Omega y \mu_p\right) \widehat{\psi}_p(y,t), \qquad t_n \le t \le t_{n+1}. \tag{137}$$

The above linear ODE can be integrated in time *exactly* and we obtain

$$\widehat{\psi}_p(y,t) = \exp\left[-i\left(\frac{1}{2}\mu_p^2 + \Omega y \mu_p\right)(t-t_n)\right]\ \widehat{\psi}_p(y,t_n), \qquad t_n \le t \le t_{n+1}. \tag{138}$$

Similarly, for each fixed x, the operator in the equation (135) is in y-direction with constant coefficients and thus we can discretize it in y-direction by a Fourier pseudospectral method. Assume

$$\psi(x,y,t) = \sum_{q=-N/2}^{N/2-1} \widehat{\psi}_q(x,t)\ \exp[i\lambda_q(y-c)], \tag{139}$$

where $\lambda_q = \frac{2q\pi}{d-c}$ and $\widehat{\psi}_q(x,t)$ is the Fourier coefficient for the q-th mode in y-direction. Plugging (139) into (135), noticing the orthogonality of the Fourier functions, we obtain for $-\frac{N}{2} \le q \le \frac{N}{2}-1$ and $a \le x \le b$:

$$i\,\partial_t \widehat{\psi}_q(x,t) = \left(\frac{1}{2}\lambda_q^2 - \Omega x \lambda_q\right) \widehat{\psi}_q(x,t), \qquad t_n \le t \le t_{n+1}. \tag{140}$$

Again the above linear ODE can be integrated in time *exactly* and we obtain

$$\widehat{\psi}_q(x,t) = \exp\left[-i\left(\frac{1}{2}\lambda_q^2 - \Omega x \lambda_q\right)(t-t_n)\right]\ \widehat{\psi}_q(x,t_n), \qquad t_n \le t \le t_{n+1}. \tag{141}$$

From time $t = t_n$ to $t = t_{n+1}$, we combine the splitting steps via the standard second order Strang splitting [71, 19]:

$$\begin{aligned}
\psi_{jk}^{(1)} &= \sum_{p=-M/2}^{M/2-1} e^{-i\Delta t(\mu_p^2 + 2\Omega y_k \mu_p)/4}\ \widehat{(\psi_k^n)}_p\ e^{i\mu_p(x_j-a)}, \ 0 \le j \le M, \quad 0 \le k \le N,\\
\psi_{jk}^{(2)} &= \sum_{q=-N/2}^{N/2-1} e^{-i\Delta t(\lambda_q^2 - 2\Omega x_j \lambda_q)/4}\ \widehat{(\psi_j^{(1)})}_q\ e^{i\lambda_q(y_k-c)}, \ 0 \le k \le N, \quad 0 \le j \le M,\\
\psi_{jk}^{(3)} &= e^{-i\Delta t[V(x_j,y_k)+\beta_2|\psi_{jk}^{(2)}|^2]}\ \psi_{jk}^{(2)},\\
\psi_{jk}^{(4)} &= \sum_{q=-N/2}^{N/2-1} e^{-i\Delta t(\lambda_q^2 - 2\Omega x_j \lambda_q)/4}\ \widehat{(\psi_j^{(3)})}_q\ e^{i\lambda_q(y_k-c)}, \ 0 \le k \le N, \quad 0 \le j \le M,\\
\psi_{jk}^{n+1} &= \sum_{p=-M/2}^{M/2-1} e^{-i\Delta t(\mu_p^2 + 2\Omega y_k \mu_p)/4}\ \widehat{(\psi_k^{(4)})}_p\ e^{i\mu_p(x_j-a)},
\end{aligned} \tag{142}$$

where for each fixed k, $\widehat{(\psi_k^\alpha)}_p$ $(p = -M/2, \cdots, M/2-1)$ with α an index, the Fourier coefficients of the vector $\psi_k^\alpha = (\psi_{0k}^\alpha,\ \psi_{1k}^\alpha,\ \cdots,\ \psi_{(M-1)k}^\alpha)^T$, are defined as

$$\widehat{(\psi_k^\alpha)}_p = \frac{1}{M}\sum_{j=0}^{M-1} \psi_{jk}^\alpha \; e^{-i\mu_p(x_j-a)}, \quad p=-\frac{M}{2},\cdots,\frac{M}{2}-1; \tag{143}$$

similarly, for each fixed j, $\widehat{(\psi_j^\alpha)}_q$ $(q=-N/1,\cdots,N/2-1)$, the Fourier coefficients of the vector $\psi_j^\alpha=(\psi_{j0}^\alpha,\,\psi_{j1}^\alpha,\,\cdots,\,\psi_{j(N-1)}^\alpha)^T$, are defined as

$$\widehat{(\psi_j^\alpha)}_q = \frac{1}{N}\sum_{k=0}^{N-1} \psi_{jk}^\alpha \; e^{-i\lambda_q(y_k-c)}, \quad q=-\frac{N}{2},\cdots,\frac{N}{2}-1. \tag{144}$$

For the above algorithm (142), the total memory requirement is $O(MN)$ and the total computational cost per time step is $O(MN\ln(MN))$. The scheme is time reversible when $W(\mathbf{x})\equiv 0$, just as it holds for the GPE (8), i.e. the scheme is unchanged if we interchange $n\leftrightarrow n+1$ and $\Delta t\leftrightarrow -\Delta t$ in (142). Also, a main advantage of the numerical method is its time-transverse invariance when $W(\mathbf{x})\equiv 0$, just as it holds for the GPE (8) itself. If a constant α is added to the external potential V, then the discrete wave functions ψ_{jk}^{n+1} obtained from (142) get multiplied by the phase factor $e^{-i\alpha(n+1)\Delta t}$, which leaves the discrete quadratic observable $|\psi_{jk}^{n+1}|^2$ unchanged. This method was demonstrated to be spectral accuracy in space and second accuracy in time [19]

6.4 The leap-frog spectral method

Another way to discretize (117) is the leap-frog spectral method. we choose $\Omega_{\mathbf{x}}=[a,b]\times[c,d]$ in 2D, and resp., $\Omega_{\mathbf{x}}=[a,b]\times[c,d]\times[e,f]$ in 3D, with $|a|$, b, $|c|$, d, $|e|$ and f sufficiently large. Again, for simplicity of notation, here we assume $\lambda=0$ and $V(\mathbf{x},t)=V(\mathbf{x})$ in (117). When $d=2$, choose spatial mesh sizes $\Delta x=(b-a)/J$ and $\Delta y=(d-c)/K$ with J, K and L even integers, denote the grid points as

$$x_j=a+j\Delta x, \quad j=0,1,\cdots,J, \qquad y_k=c+k\Delta y, \quad k=0,1,\cdots,K.$$

let $\psi_{j,k}^n$ be the approximation of $\psi(x_j,y_k,t_n)$. For $n=1,2,\cdots$, from time $t=t_{n-1}=(n-1)\Delta t$ to $t=t_{n+1}=t_n+\Delta t$, the GPE (112) is discretized in space by the Fourier pseudospectral method and in time by the leap-frog scheme, i.e. for $j=0,1,\cdots,J$ and $k=0,1,\cdots,K$

$$i\frac{\psi_{j,k}^{n+1}-\psi_{j,k}^{n-1}}{2\Delta t} = -\frac{1}{2}\left.\left(\nabla_h^2\psi^n\right)\right|_{j,k} + V_2(x_j,y_k)\psi_{j,k}^n + \beta_2|\psi_{j,k}^n|^2\psi_{j,k}^n - \Omega\left.\left(L_h\psi^n\right)\right|_{j,k}, \tag{145}$$

where ∇_h^2 and L_h, the pseudospectral differential operator approximating the operators ∇^2 and L_z respectively, are defined as

$$\left(\nabla_h^2 \psi^n\right)\big|_{j,k} = -\sum_{p=-J/2}^{J/2-1} \sum_{q=-K/2}^{K/2-1} \left(\mu_p^2 + \lambda_q^2\right) \widehat{(\psi^n)}_{p,q}\, e^{i\mu_p(x_j-a)}\, e^{i\lambda_q(y_k-c)},$$

$$\left(L_h \psi^n\right)\big|_{j,k} = x_j \left(D_y^h \psi^n\right)\big|_{j,k} - y_k \left(D_x^h \psi^n\right)\big|_{j,k}, \quad 0 \le j \le J,\ 0 \le k \le K,$$

$$\left(D_x^h \psi^n\right)\big|_{j,k} = \sum_{p=-J/2}^{J/2-1} \sum_{q=-K/2}^{K/2-1} \mu_p\, \widehat{(\psi^n)}_{p,q}\, e^{i\mu_p(x_j-a)}\, e^{i\lambda_q(y_k-c)},$$

$$\left(D_y^h \psi^n\right)\big|_{j,k} = \sum_{p=-J/2}^{J/2-1} \sum_{q=-K/2}^{K/2-1} \lambda_q\, \widehat{(\psi^n)}_{p,q}\, e^{i\mu_p(x_j-a)}\, e^{i\lambda_q(y_k-c)},$$

with

$$\mu_p = \frac{2p\pi}{b-a}, \quad p = -\frac{J}{2}, \cdots, \frac{J}{2}-1; \qquad \lambda_q = \frac{2q\pi}{d-c}, \quad q = -\frac{K}{2}, \cdots, \frac{K}{2}-1,$$

$$\widehat{(\psi^n)}_{p,q} = \frac{1}{JK} \sum_{j=0}^{J-1} \sum_{k=0}^{K-1} \psi_{j,k}^n\, e^{-i\mu_p(x_j-a)}\, e^{-i\lambda_q(y_k-c)}.$$

As stated in the introduction, here we use the leap-frog scheme for time discretization since we want to have an explicit and time reversible time integrator. In order to compute $\psi_{j,k}^1$, we apply the modified trapezoidal rule in time on the interval $[t_0, t_1]$:

$$i\frac{\psi_{j,k}^{(1)} - \psi_{j,k}^0}{\Delta t} = -\frac{1}{2}\left(\nabla_h^2 \psi^0\right)\big|_{j,k} + V_2(x_j, y_k)\psi_{j,k}^0 + \beta_2|\psi_{j,k}^0|^2\psi_{j,k}^0 - \Omega\left(L_h \psi^0\right)\big|_{j,k},$$

$$i\frac{\psi_{j,k}^{(2)} - \psi_{j,k}^{(1)}}{\Delta t} = -\frac{1}{2}\left(\nabla_h^2 \psi^{(1)}\right)\big|_{j,k} + V_2(x_j, y_k)\psi_{j,k}^{(1)} + \beta_2|\psi_{j,k}^{(1)}|^2\psi_{j,k}^{(1)} - \Omega\left(L_h \psi^{(1)}\right)\big|_{j,k},$$

$$\psi_{j,k}^1 = \frac{1}{2}\left(\psi_{j,k}^{(1)} + \psi_{j,k}^{(2)}\right), \qquad j = 0, 1, \cdots, J,\ k = 0, 1, \cdots, K. \tag{146}$$

The initial data (119) is discretized as

$$\psi_{j,k}^0 = \psi_0(x_j, y_k), \qquad j = 0, 1, \cdots, J, \quad k = 0, 1, \cdots, K. \tag{147}$$

The leap-frog Fourier pseudospectral discretization (145) is explicit and time reversible. The total memory requirement is $O(JK)$ and the total computational cost per time step is $O(JK\ln(JK))$. Following the standard von Neumann analysis and coefficient frozen technique, the stability condition for (145) is

$$\Delta t < \frac{2(\Delta x)^2}{\pi^2\left[1 + \left(\frac{\Delta x}{\Delta y}\right)^2\right] + \max_{\mathbf{x}\in\Omega_{\mathbf{x}}}\left[\pi\left(|x|\Delta x + |y|\frac{(\Delta x)^2}{\Delta y}\right) + V_2(\mathbf{x}) + \beta_2|\psi(\mathbf{x}, t)|^2\right]}.$$

This method was demonstrated to be spectral accuracy in space and second accuracy in time [77]

6.5 Numerical results

Many numerical results were reported in [10, 19, 77] to demonstrate the efficiency and accuracy of the above numerical methods. Here we only report the dynamics of a quantized vortex lattice with 81 vortices in rotating BEC. We take $d = 2$, $\beta_2 = 2000$, $\Omega = 0.9$. The initial condition in (119) is taken as the ground state [20, 10, 6] of the GPE computed numerically with the the same parameter values and $\gamma_x = \gamma_y = 1$. Then at $t = 0$, we change the trap frequency by setting $\gamma_x = \gamma_y = 1.5$, or $\gamma_x = 1.2$ and $\gamma_y = 1.5$ respectively. We take $\Omega_{\mathbf{x}} = [-24, 24] \times [-24, 24]$ and choose mesh size $\Delta x = \Delta y = 3/64$ and time step $\Delta = 0.0001$. Figures 3-4 show contour plots of the density function $|\psi(\mathbf{x}, t)|^2$ at different times.

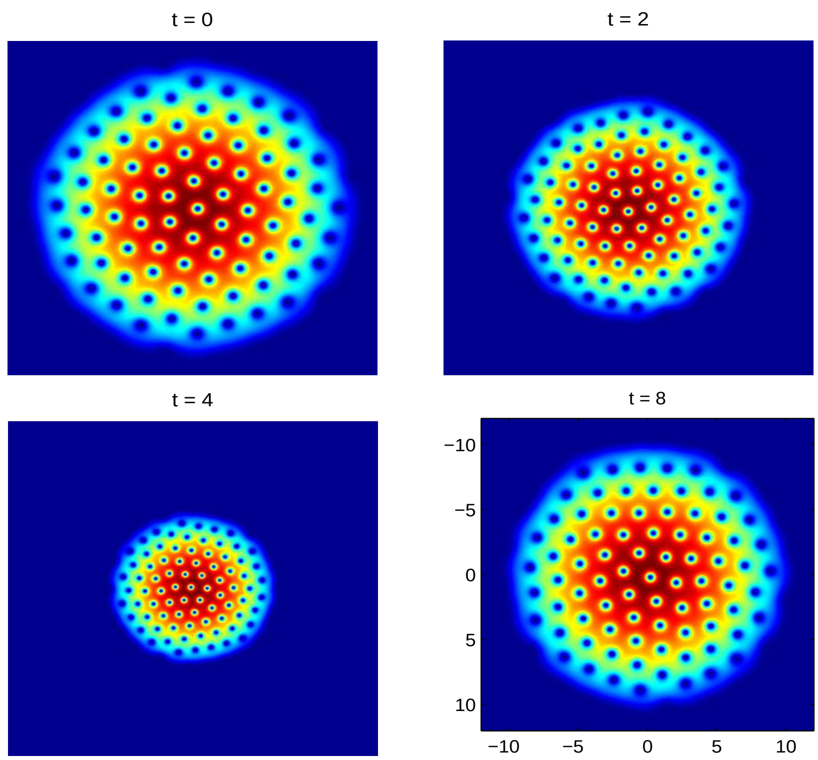

Fig. 3. The contour plots of the density function $|\psi(\mathbf{x}, t)|$ of the vortex lattices at different time for changing from $\gamma_x = \gamma_y = 1$ to $\gamma_x = \gamma_y = 1.5$.

From Figs. 3-4, at $t = 0$, there are 81 quantized vortices in the ground state. During the time evolution, the lattice is rotated due to the angular momentum term (cf. Fig. 4), and shrunk or expanded due to the changing

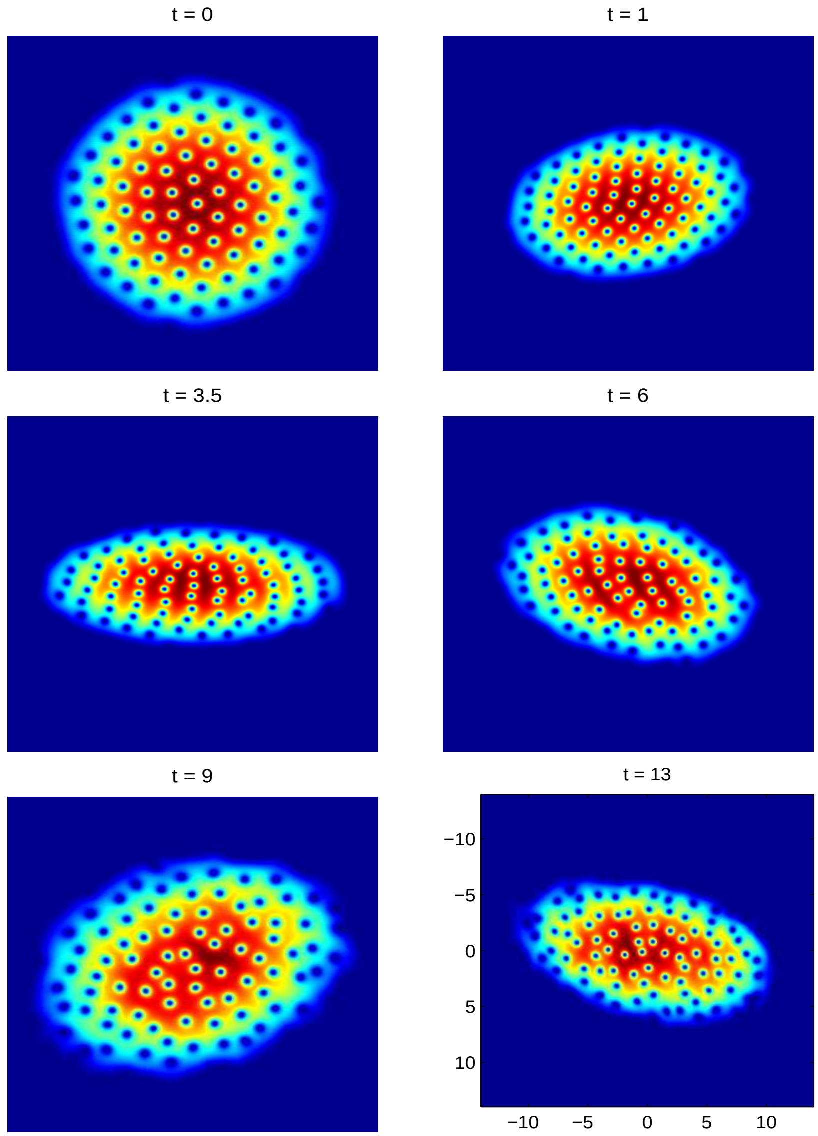

Fig. 4. The contour plots of the density function $|\psi(\mathbf{x},t)|$ of the vortex lattices at different time for changing from $\gamma_x = \gamma_y = 1$ to $\gamma_x = 1.2$ and $\gamma_y = 1.5$.

of the trapping frequencies (cf. Fig. 3). This clearly demonstrates the high resolution of the LFFP method for rotating BEC.

7 Conclusion

We have reviewed our recent works for the ground state and dynamics of the Gross-Pitaevskii equation with an angular momentum rotation term for rotating BECs. Along the analytical front, we provided asymptotics of the energy and chemical potential of the ground state in the semiclassical regime, showed that the ground state is a global minimizer of the energy functional over the unit sphere and all excited states are saddle points in the linear case. We proved the conservation of the angular momentum expectation when the external trapping potential is radially symmetric in 2D, and respectively cylindrically symmetric in 3D. A second-order ODE was also derived to describe the time-evolution of the condensate width as a periodic function with/without a perturbation, and the frequency of the periodic function doubles the trapping frequency. We also presented an ODE system with a complete initial data that governs the dynamics of a stationary state with a shifted center and we also illustrated the decrease in the total density when a damping term is applied in the GPE. On the numerical side, we reviewed the continuous normalized gradient flow with backward Euler finite difference discretization for computing ground state in rotating BEC and three efficient and accurate numerical method for computing the dynamics of rotating BEC. Finally the dynamics of a quantized vortex lattice with **81** vortices is reported to demonstrate the spectral resolution of our numerical methods.

Acknowledgment

The author thanks his collaborators Peter A. Markowich, Qiang Du, Yanzhi Zhang and Hanquan Wang for very fruitful collaboration in this subject and acknowledges support by the National University of Singapore grant No. R-146-000-081-112.

References

1. J. R. Abo-Shaeer, C. Raman, J. M. Vogels, and W. Ketterle, *Observation of vortex lattices in Bose-Einstein condensates*, Science, 292 (2001), pp. 476.
2. S. K. Adhikari and P. Muruganandam, *Effect of an implusive force on vortices in a rotating Bose-Einstein condensate*, Phys. Lett. A, 301 (2002), pp. 333-339.
3. A. Aftalion and Q. Du, *Vortices in a rotating Bose-Einstein condensate: critical angular velocities and energy diagrams in the Thomas-Fermi regime*, Phys. Rev. A, 64 (2001), article 063603.
4. A. Aftalion, Q. Du and Y. Pomeau, *Dissipative flow and vortex shedding in the Painlevé boundary layer of a Bose Einstein condensate*, Phy. Rev. Lett., 91 (2003), aritcle 090407.

5. A. Aftalion and T. Riviere, *Vortex energy and vortex bending for a rotating Bose-Einstein condensate*, Phys. Rev. A, 64 (2001), 043611.
6. A. Aftalion and I. Danaila, *Three-dimensional vortex configurations in a rotating Bose Einstein condensate*, Phys. Rev. A, 68 (2003), 023603.
7. M. H. Anderson, J.R. Ensher, M.R. Matthews, C.E. Wieman, and E.A. Cornell, *Observation of Bose-Einstein Condensation in a Dilute Atomic Vapor*, Science, 269 (1995), 198.
8. W. Bao, *Ground states and dynamics of multi-component Bose-Einstein condensates*, Multiscale Modeling and Simulation, 2 (2004), pp. 210-236.
9. W. Bao and Q. Du, *Computing the ground state solution of Bose-Einstein condensates by a normalized gradient flow*, SIAM J. Sci. Comput., 25 (2004), pp. 1674-1697.
10. W. Bao, Q. Du and Y. Zhang, *Dynamics of rotating Bose-Einstein condensates and their efficient and accurate numerical computation*, SIAM J. Appl. Math., 66 (2006), pp. 758-786.
11. W. Bao, D. Jaksch, *An explicit unconditionally stable numerical methods for solving damped nonlinear Schrödinger equations with a focusing nonlinearity*, SIAM J. Numer. Anal., 41 (2003), pp. 1406-1426.
12. W. Bao, D. Jaksch and P.A. Markowich, *Numerical solution of the Gross-Pitaevskii Equation for Bose-Einstein condensation*, J. Comput. Phys., 187 (2003), pp. 318 - 342.
13. W. Bao, D. Jaksch and P.A. Markowich, *Three dimensional simulation of jet formation in collapsing condensates*, J. Phys. B: At. Mol. Opt. Phys., 37 (2004), pp. 329-343.
14. W. Bao, S. Jin and P. A. Markowich, *On time-splitting spectral approximation for the Schrödinger equation in the semiclassical regime*, J. Comput. Phys., 175 (2002), pp. 487-524.
15. W. Bao, S. Jin and P. A. Markowich, *Numerical study of time-splitting spectral discretizations of nonlinear Schrödinger equations in the semi-classical regimes*, SIAM J. Sci. Comput., 25 (2003), pp. 27-64.
16. W. Bao, F.Y. Lim and Y. Zhang, *Energy and chemical potential asymptotics for the ground state of Bose-Einstein condensates in the semiclassical regime*, Trans. Theory Stat. Phys., to appear.
17. W. Bao and J. Shen, *A fourth-order time-splitting Laguerre-Hermite pseudo-spectral method for Bose-Einstein condensates*, SIAM J. Sci. Comput., 26 (2005), pp. 2010-2028.
18. W. Bao and W. Tang, *Ground state solution of trapped interacting Bose-Einstein condensate by directly minimizing the energy functional*, J. Comput. Phys., 187 (2003), pp. 230-254.
19. W. Bao and H. Wang, *An efficient and spectrally accurate numerical method for computing dynamics of rotating Bose-Einstein condensates*, J. Comput. Phys., to appear.
20. W. Bao, H. Wang and P.A. Markowich, *Ground, symmetric and central vortex states in rotating Bose-Einstein condensates*, Comm. Math. Sci., 3 (2005), pp. 57-88.
21. W. Bao and Y. Zhang, *Dynamics of the ground state and central vortec states in Bose-Einstein condensation*, Math. Mod. Meth. Appl. Sci., 15 (2005), pp. 1863-1896.

22. I. Bialynicki-Birula and Z. Bialynicki-Birula, *Center-of-mass motion in the many-body theory of Bose-Einstein condensates*, Phys. Rev. A, 65 (2002), article 063606.
23. C. C. Bradley, C.A. Sackett, R.G. Hulet, *Evidence of Bose-Einstein condensation in an atomic gas with attractive interactions*, Phys. Rev. Lett., 75 (1995), 1687.
24. Y. Castin and R. Dum, *Bose-Einstein condensates with vortices in rotating traps*, Eur. Phys. J. D, 7 (1999), pp. 399-412.
25. B. M. Caradoc-Davis, R. J. Ballagh and P. B. Blakie, *Three-dimensional vortex dynamics in Bose-Einstein condensates*, Phys. Rev. A, 62 (2000), 011602.
26. B. M. Caradoc-Davis, R. J. Ballagh and P. B. Blakie, *Coherent dynamics of vortex formation in trapped Bose-Einstein condensates*, Phys. Rev. Lett., 83 (1999), 895.
27. M. M, Cerimele, M. L. Chiofalo, F. Pistella, S. Succi and M. P. Tosi, *Numerical solution of the Gross-Pitaevskii equation using an explicit finite-difference scheme: An application to trapped Bose-Einstein condensates*, Phys. Rev. E, 62 (2000), pp. 1382-1389.
28. M. M, Cerimele, F. Pistella and S. Succi, *Particle-inspired scheme for the Gross-Pitaevskii equation: An application to Bose-Einstein condensation*, Comput. Phys. Comm., 129 (2000), pp. 82-90.
29. S.-M. Chang, W.-W. Lin and S.-F., Shieh, *Gauss-Seidel-type methods for energy states of a multi-component Bose-Einstein condensate*, J. Comput. Phys., to appear.
30. M. L. Chiofalo, S. Succi and M.P. Tosi, *Ground state of trapped interacting Bose-Einstein condensates by an explicit imaginary-time algorithm*, Phys. Rev. E, 62 (2000), 7438.
31. F. Dalfovo and S. Giorgini, *Theory of Bose-Einstein condensation in trapped gases*, Rev. Mod. Phys., 71 (1999), 463.
32. K. B. Davis, M.O. Mewes, M.R. Andrews, N.J. van Druten, D.S. Durfee, D.M. Kurn, and W. Ketterle, *Bose-Einstein Condensation in a gas of Sodium atoms*, Phys. Rev. Lett., 75 (1995), 3969.
33. R. J. Donnelly, *Quantizied vortices in Helium II*, Cambridge University Press, 1991.
34. P. Engels, I. Coddington, P. Haijan and E. Cornell, *Nonequilibrium effects of anisotropic compression applied to vortex lattices in Bose-Einstein condendates*, Phy. Rev. Lett, 89 (2002), article 100403.
35. J. R. Ensher, D. S. Jin, M. R. Matthews, C. E. Wieman and E. A. Cornell, *Bose-Einstein Condensation in a Dilute Gas: Measurement of Energy and Ground-State Occupation*, Phys. Rev. Lett., 77 (1996), 4984.
36. D. L. Feder, C. W. Clark and B. I. Schneider, *Nucleation of vortex arrays in rotating anisotropic Bose-Einstein condensates*, Phys. Rev. A, 61 (1999), 011601.
37. D. L. Feder, C. W. Clark and B. I. Schneider, *Vortex stability of interacting Bose-Einstein condensates confined in anisotropic harmonic traps*, Phys. Rev. Lett., 82 (1999), 4956.
38. D. L. Feder, A. A. Svidzinsky, A. L. Fetter and C. W. Clark, *Anomalous modes drive vortex dynamics in confined Bose-Einstein condensates*, Phys. Rev. Lett., 86 (2001), pp. 564-567.

39. A. L. Fetter and A. A. Svidzinsky, *Vortices in a trapped dilute Bose-Einstein condensate*, J. Phys. Condens. Matter, 13 (2001), R135-194.
40. J. J. Garcia-Ripoll and V. M. Perez-Garcia and V. Vekslerchik, *Construction of exact solutions by spatial translations in inhomogeneous nonlinear Schrödinger equations*, Phys. Rev. E, 64 (2001), article 056602.
41. R. Glowinski and P. LeTallec, *Augmented Lagrangians and Operator Splitting Methods in Nonlinear Mechanics*, SIAM, Philadelphia, 1989.
42. E. P. Gross, Nuovo. Cimento., 20 (1961), pp. 454.
43. D. S. Hall, M. R. Mattthews, J. R. Ensher, C. E. Wieman and E. A. Cornell, *Dynamics of component separation in a binary mixture of Bose-Einstein condensates*, Phys. Rev. Lett., 81 (1998), pp. 1539-1542.
44. J.J. Garcia-Ripoll, V.M. Perez-Garcia, *Vortex bending and tightly packed vortex latices in Bose-Einstein condensates*, Phys. Rev. A, to appear.
45. J. J. Garcia-Ripoll and V. M. Perez-Garcia, *Stability of vortices in inhomogeneous Bose Einstein condensates subject to rotation: A three dimensional analysis*, Phys. Rev. A, 60 (1999), pp. 4864-4874.
46. J. J. Garcia-Ripoll and V. M. Perez-Garcia, *Optimizing Schrödinger functionals using Sobolev gradients: application to quantum mechanics and nonlinear optics*, SIAM J. Sci. Comput., 23 (2001), pp. 1316-1334.
47. J.J. Garcia-Ripoll and V. M. Perez-Garcia, *Vortex nucleation and hysteresis phenomena in rotating Bose-Einstein condensate*, Phys. Rev. A, 63 (2001), 041603.
48. B. Jackson, J. F. McCann and C. S. Adams, *Vortex formation in dilute inhomogeneous Bose-Einstein Condensates*, Phys. Rev. Lett., 80 (1998), 3903.
49. B. Jackson, J. F. McCann and C. S. Adams, *Vortex line and ring dynamics in trapped Bose-Einstein condensates*, Phys. Rev. A, 61 (1999), 013604.
50. D. Jaksch, C. Bruder, J. I. Cirac, C. W. Gardiner and P. Zoller, *Cold bosonic atoms in optical lattices*, Phys. Rev. Lett., 81 (1998), pp. 3108-3111.
51. K. Kasamatsu, M. Tsubota and M. Ueda, *Nonlinear dynamics of vortex lattice formation in a rotating Bose- Einstein condensate*, Phys. Rev. A, 67 (2003), article 033610.
52. L. Laudau and E. Lifschitz, *Quantum Mechanics: non-relativistic theory*, Pergamon Press, New York, 1977.
53. E. H. Lieb, R. Seiringer and J. Yngvason, *Bosons in a Trap: A Rigorous Derivation of the Gross-Pitaevskii Energy Functional*, Phys. Rev. A, 61 (2000), 3602.
54. E. M. Lifshitz and L. P. Pitaevskii, *Statistical Physics*, 3rd edition, Pergamon, Oxford, 1980.
55. E. Lundh, C.J. Pethick and H. Smith, *Vortices in Bose-Einstein-condensated atomic clouds*, Phys. Rev. A, 58 (1998), 4816-4823.
56. K. W. Madison, F. Chevy, W. Wohlleben and J. Dalibard, *Vortex formation in a stirred Bose-Einstein Condensate*, Phys. Rev. Lett., 84 (2000), 806.
57. M. R. Matthews, B. P. Anderson, P. C. Haljan, D. S. Hall, C. E. Wieman and E. A. Cornell, *Vortices in a Bose-Einstein Condensate*, Phys. Rev. Lett., 83 (1999), 2498.
58. A. Minguzzi, S. Succi, F. Toschi, M. P. Tosi, P. Vignolo, *Numerical methods for atomic quantum gases with applications to Bose-Einstein condensates and to ultracold fermions*, Phys. Rep., 395 (2004), pp. 223-355.

59. M. Modugno, L. Pricoupenko and Y. Castin, *Bose-Einstein condensates with a bent vortex in rotating traps*, Eur. Phys. J. D, 22 (2003), pp. 235-257.
60. L. P. Pitaevskii, *Vortex lines in a imperfect Bose gas*, Zh. Eksp. Teor. Fiz., 40 (1961), 646. (Sov. Phys. JETP, 13 (1961), 451).
61. L. Pitaevskii and S. Stringari, *Bose-Einstein condensation*, Oxford, New York, Clarendon Press, 2003.
62. A. A. Penckwitt and R.J. Ballagh, *The nucleation, growth and stabilization of vortex lattices*, cond-mat/0205037.
63. C. J. Pethick and H. Smith, *Bose-Einstein condensation in dilute gases*, Cambridge University Press, 2002.
64. L. P. Pitaevskii and S. Stringari, *Bose-Einstein condensation*, Clarendon Press, 2003.
65. C. Raman, J. R. Abo-Shaeer, J. M. Vogels, K. Xu and W. Ketterle, *Vortex nucleation in a stirred Bose-Einstein Condensate*, Phys. Rev. Lett., 87 (2001), 210402.
66. P. Rosenbuch, V. Bretin and J. Dalibard, Phys. Rev. lett., 89 (2002), 200403.
67. R. Seiringer, *Gross-Pitaevskii theory of the rotating Bose gas*, Comm. Math. Phys., 229 (2002), pp. 491-509.
68. R. Seiringer, *Ground state asymptotics of a dilute rotating gas*, J. Phys. A: Math. Gen., 36 (2003), pp. 9755-9778.
69. T.P. Simula, P. Engels, I. Coddington, V. Schweikhard, E.A. Cornell and R.J. Ballagh, *Observations on sound propagation in rapidly rotating Bose-Einstein condensates*, cond-mat/0407343.
70. T.P. Simula, A.A. Penckwitt and R.J. Ballagh, *Giant vortex lattice deformations in rapidly rotating Bose-Einstein condensates*, cond-mat/0307130.
71. G. Strang, *On the construction and comparison of difference schemes*, SIAM J. Numer. Anal., 5 (1968), pp. 505-517.
72. A. A. Svidzinsky and A. L. Fetter, *Dynamics of a vortex in a trapped Bose-Einstein condensate*, Phys. Rev. A, 62 (2000), 063617.
73. L. Simon, *Asymptotics for a class of nonlinear evolution equations, with applications to geometric problems*, Ann. Math., 118 (1983), pp. 525-571.
74. S. Sinha and Y. Castin, *Dynamic instability of a rotating Bose-Einstein condensate*, Phys. Rev. Lett., 87 (2001), 190402.
75. M. Tsubota, K. Kasamatsu and M. Ueda, *Vortex lattice formation in a rotating Bose-Einstein condensate*, Phys. Rev. A, 65 (2000), 023603.
76. J.E. Williams and M.J. Hooand, *Preparing topological states of a Bose-Einstein condensate*, Nature, 401 (1999), 568.
77. Y. Zhang and W. Bao, *Dynamics of the center of mass in rotating Bose-Einstein condensates*, Appl. Numer. Math., to appear.